

Realtime 4D tomographic microscopy: the SLS experience

M. Stampanoni^{a,b}
on behalf of the TOMCAT team

^aSwiss Light Source, Paul Scherrer Institut, 5232 Villigen, Switzerland;

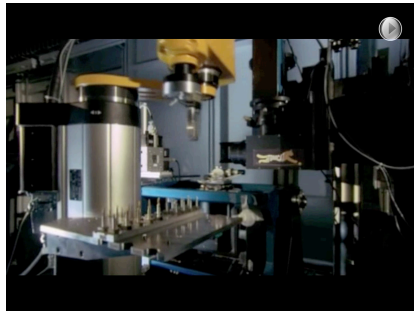
^bInstitute for Biomedical Engineering, University and ETH Zürich, 8092 Zürich, Switzerland;



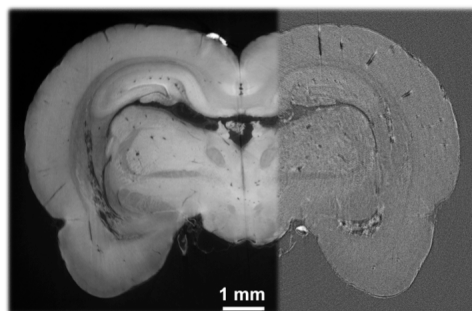
TOMCAT at a glance

Features:

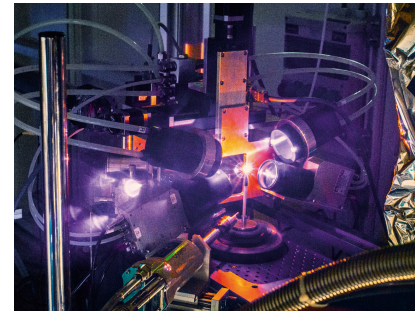
- Wide spatial resolution range: nano-to-meso scales (0.1-10 μ m)
- Broad range of sample sizes (10 μ m-20mm)
- High density resolution enhanced by phase contrast
- High temporal resolution (3D data acquisition in less than 1s)



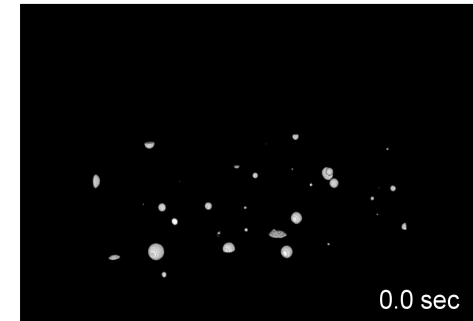
Automation
large scale
studies



Density resolution
phase contrast
imaging



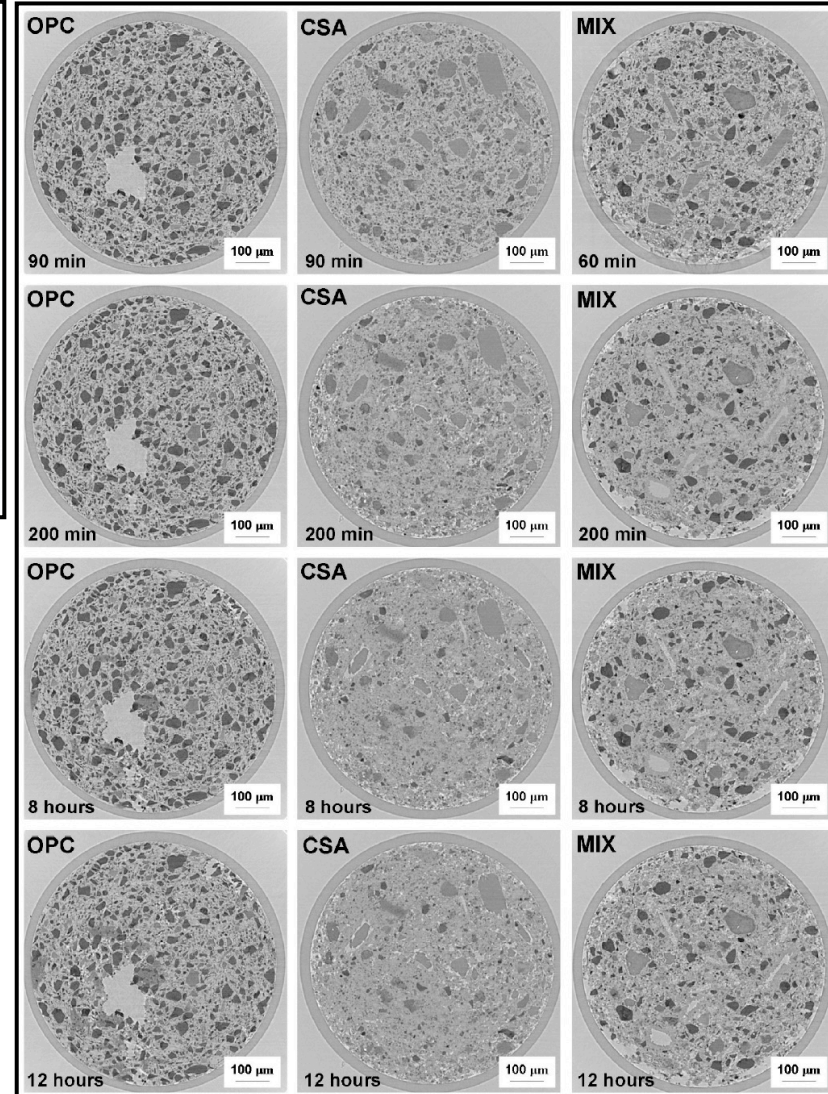
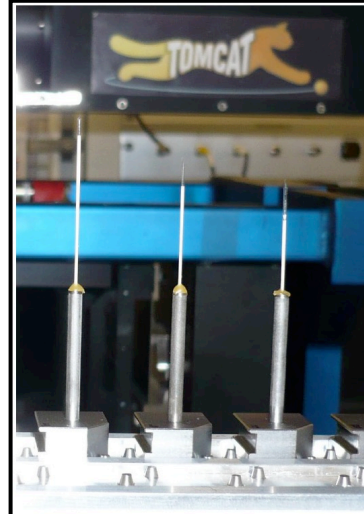
In situ
capabilities
temperatures
away from
ambient



Ultra-fast data
acquisition
dynamic studies

Fully automated tomographic microscopy endstation

D. Attenborough's "First Life", BBC 2011

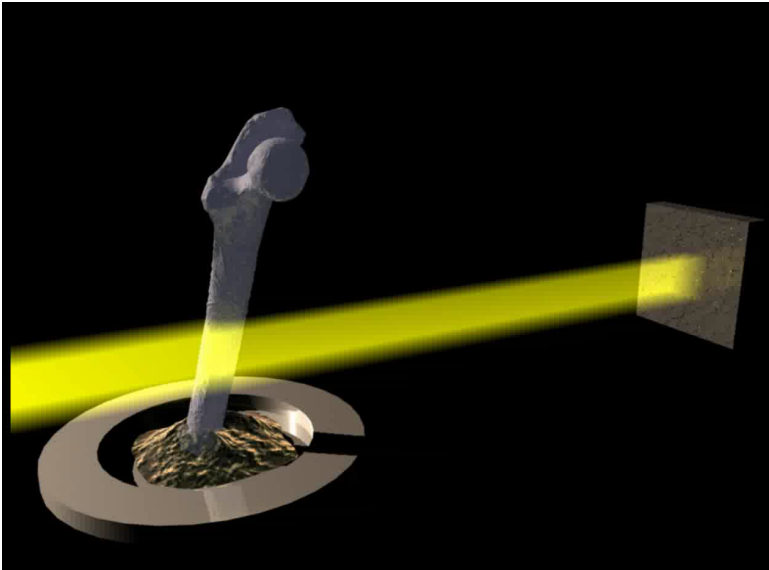


- Cement materials in capillaries of 600 microns diameter
 - Study on different binders:
 - Ordinary Portland Cement (OPC)
 - Calcium Sulphoaluminate Cement (CSA)
 - Mixed sample(MIX)
 - Sample mounting and sequencing fully automatic
- Unattended monitoring of hydration process over 12h

D. Gastaldi, Construction and Building Materials 29 (2012) 284–290

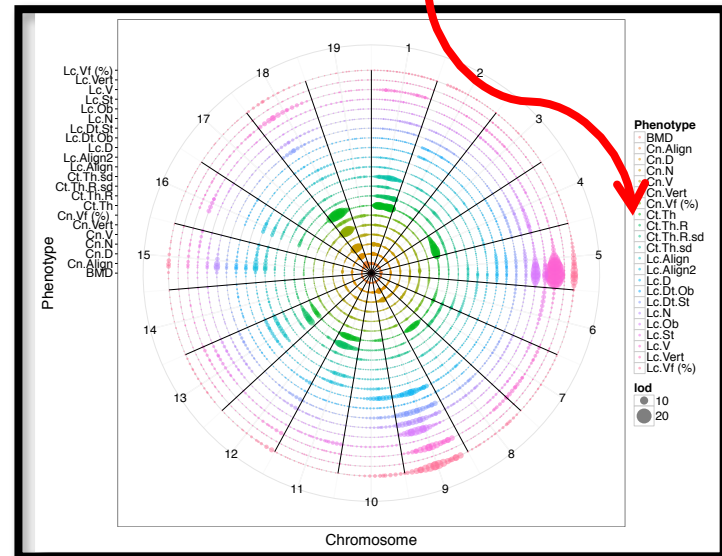
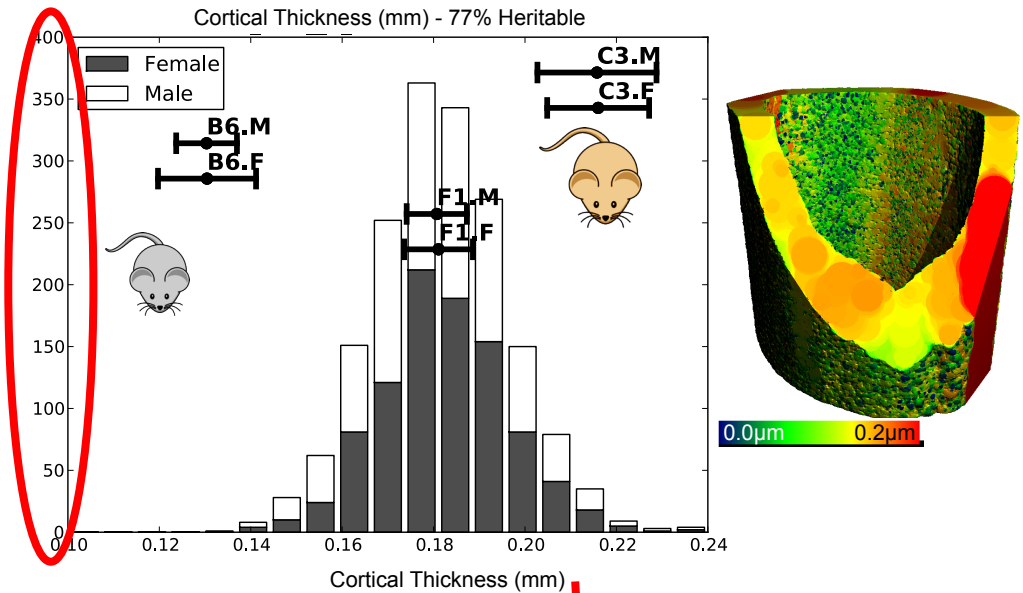
High-throughput: from sample alignment to QTL analysis

High-throughput: ROI selection and alignment



Femur samples automatically aligned using goniometer and moved to region of interest using projections and image processing scripts

One Beamtime
One PhD student
398 samples
(10 minutes/sample)



K. Mader, PhD Thesis 2013 and K. Mader et al., BMC Genomics 16:493 (03 Jul 2015)

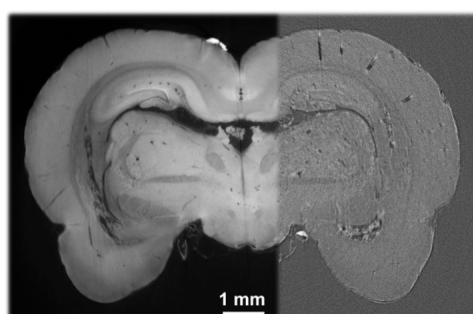
TOMCAT at a glance

Features:

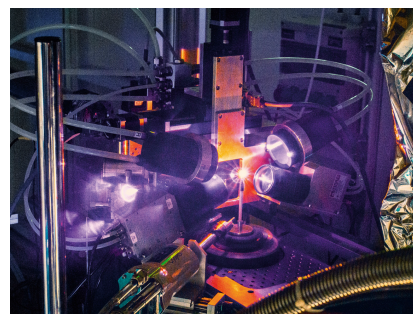
- Wide spatial resolution range: nano-to-meso scales (0.1-10 μ m)
- Broad range of sample sizes (10 μ m-20mm)
- High density resolution enhanced by phase contrast
- High temporal resolution (3D data acquisition in less than 1s)



Automation
large scale
studies



Density resolution
phase contrast
imaging



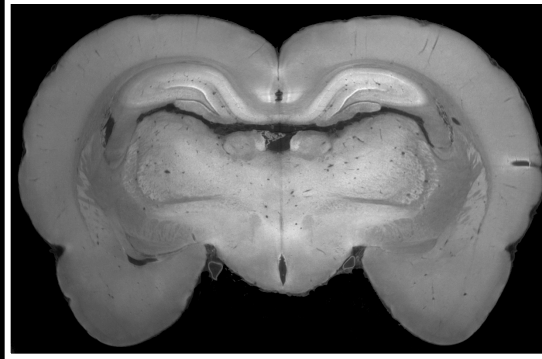
In situ
capabilities
temperatures
away from
ambient



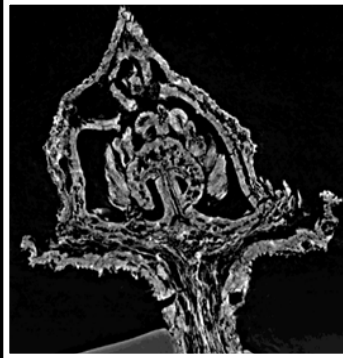
Ultra-fast data
acquisition
dynamic studies

Phase contrast imaging over four length scales

E. M. Friis, M. Stampanoni et al., Nature 2007
Modified Transport of Intensity



S. McDonald, M. Stampanoni et al., JSR 2009
Talbot interferometry



M. Stampanoni et al, PRB 2010
Hard X-ray Zernike Phase Contrast



T. Thüring et al, Skeletal Radiology, 2013
Talbot-Lau interferometry

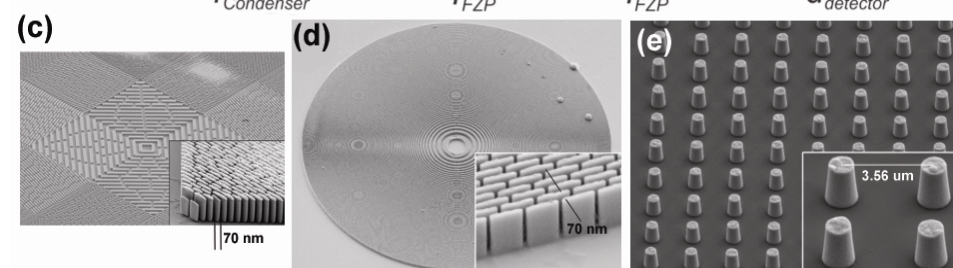
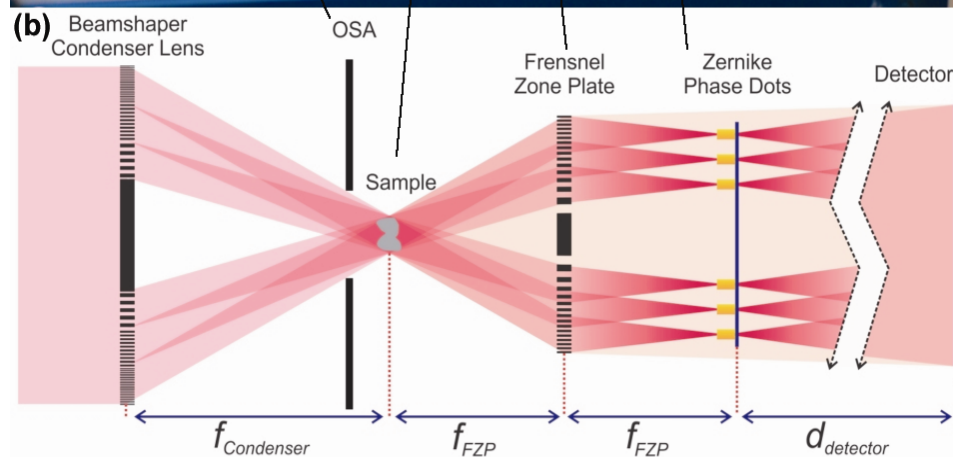
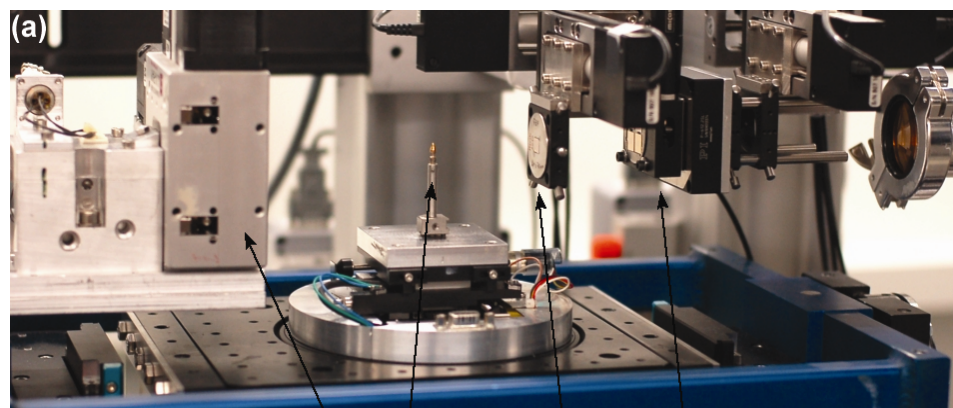
0.1 micron
cells

1 micron

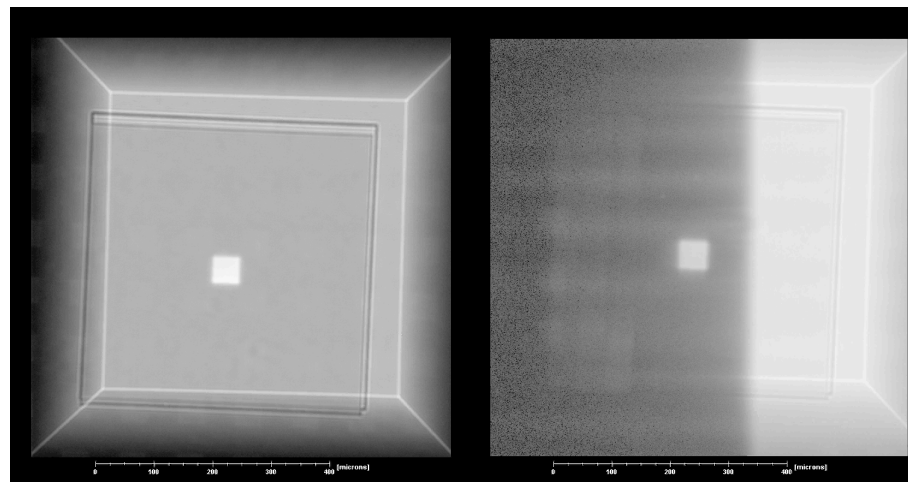
10 microns
small animals

100 microns
humans

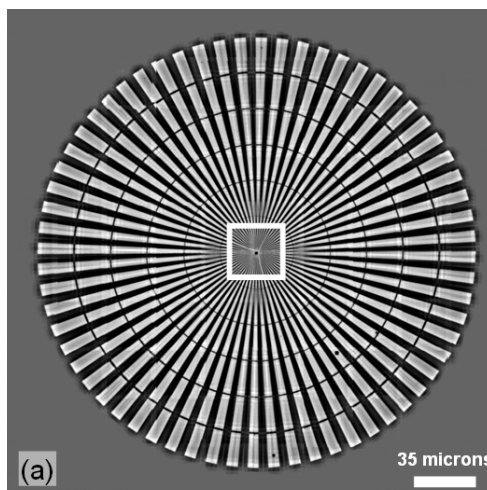
TOMCAT nanoscope (operating at 150-200nm)



Square, top-flat, illumination



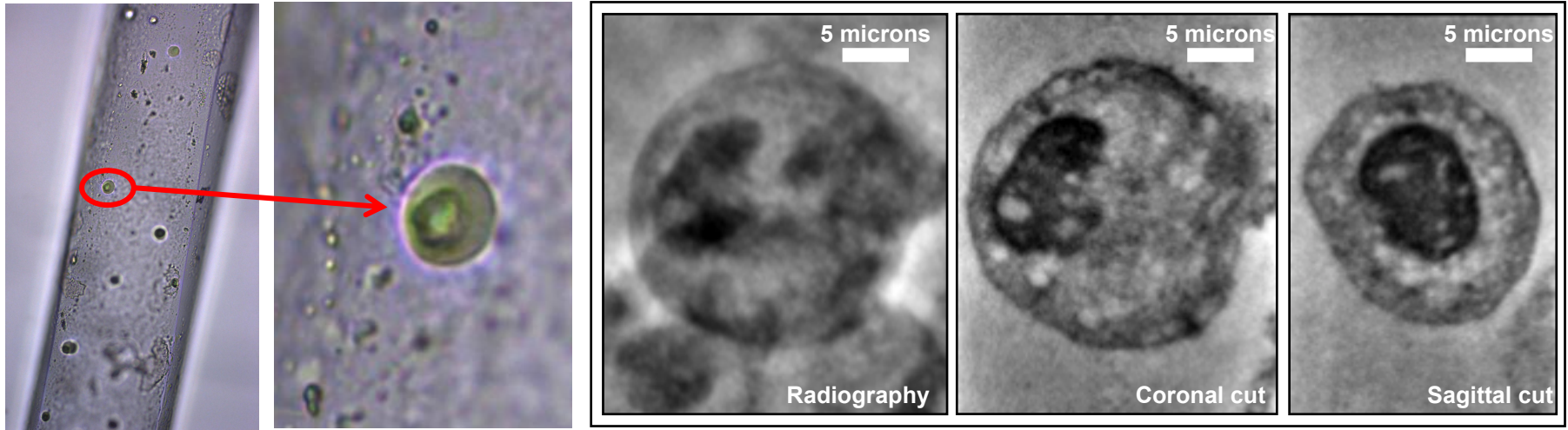
Sensitivity and resolution



Si - Siemens star

- 300 microns diameter
- 1 microns depth structure
- Phase shift: $\pi/15$
- Rayleigh limit : 122 nm
- Measured: 133 nm (2D)
- Energy: 10 keV

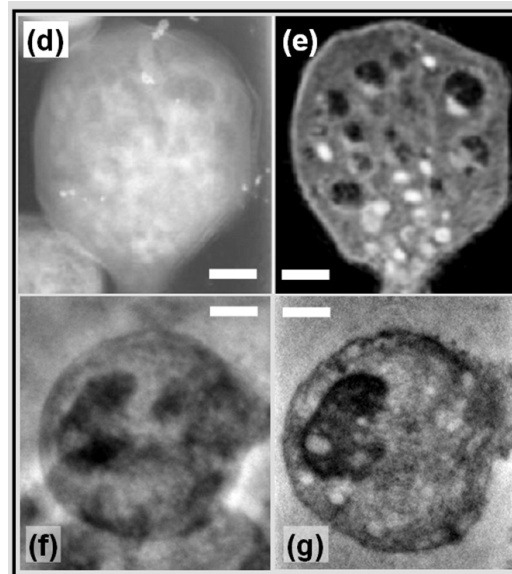
Nanotomography of a MC3-preosteoblast cell



TOMCAT Nanoscope

- 10 keV
- Pixel Size 70 nm
- True 3D res: ~ 200 nm
- High penetration power !
- High depth of focus !
- No cooling
- Sample in large capillary
- Lower dose-deposition

M. Stampanoni et al., PRB2010

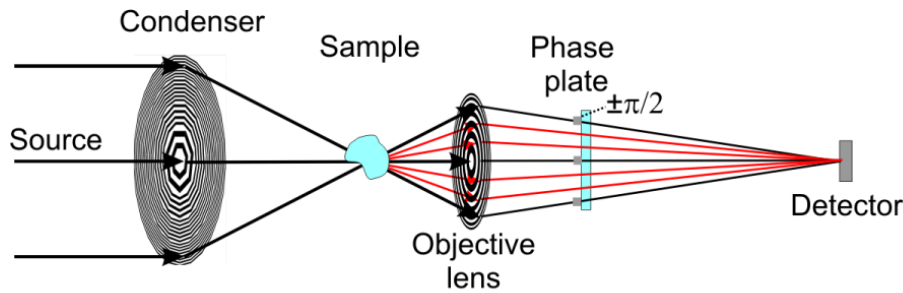


ALS: XM-1 Microscope

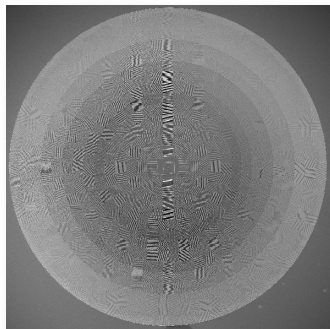
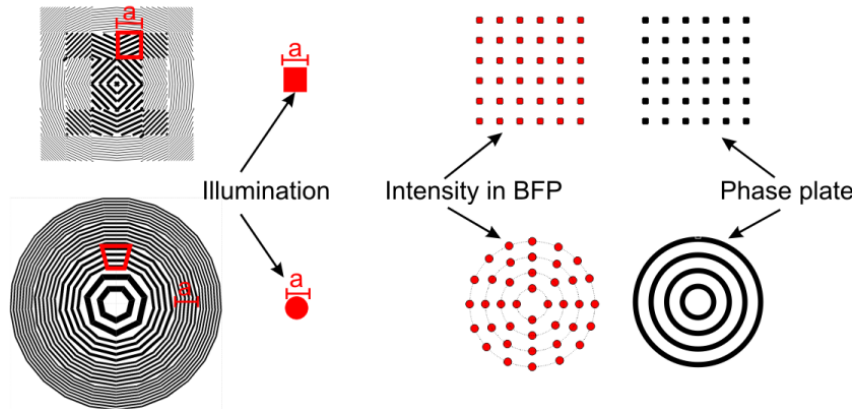
- Water window operation
- Pixel size: 50 nm
- True resolution: >100 nm
- Optics in vacuum
- Sample cryo-cooled
- Single cells in 20 microns capillary

C.A. Larabell et al., Molecular Biology of the Cell,
15(3), 956-962, 2004

Improving efficiency → faster acquisition



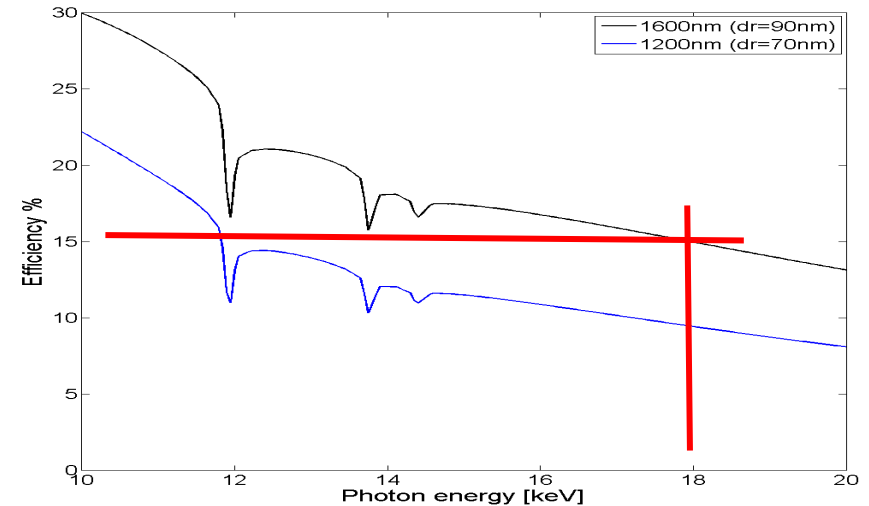
SEM-image of the FZP. Inset shows the thickness of the zones tilted at 45 degrees.



SEM-image of the condenser.

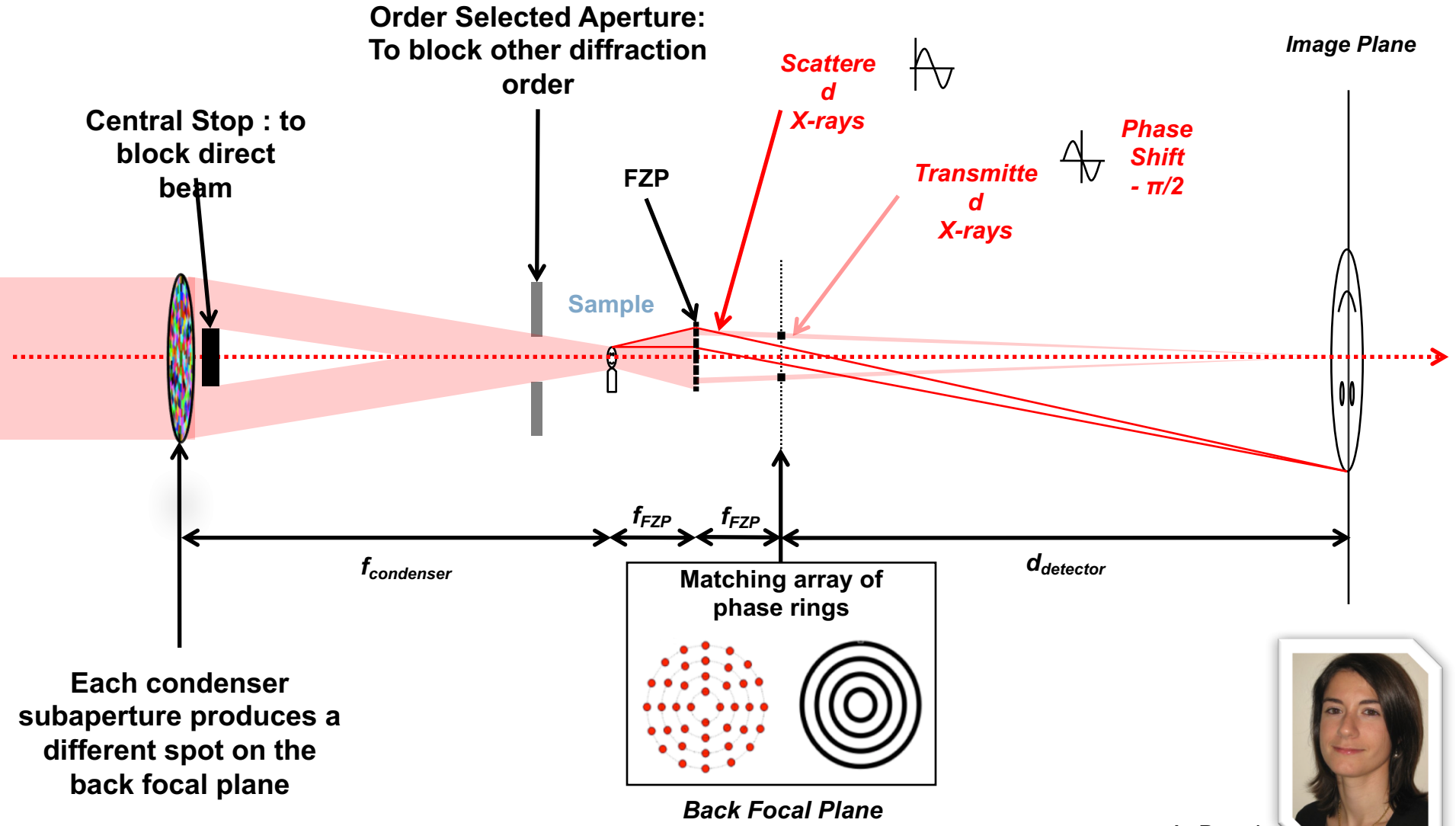


SEM-image of the phase rings.



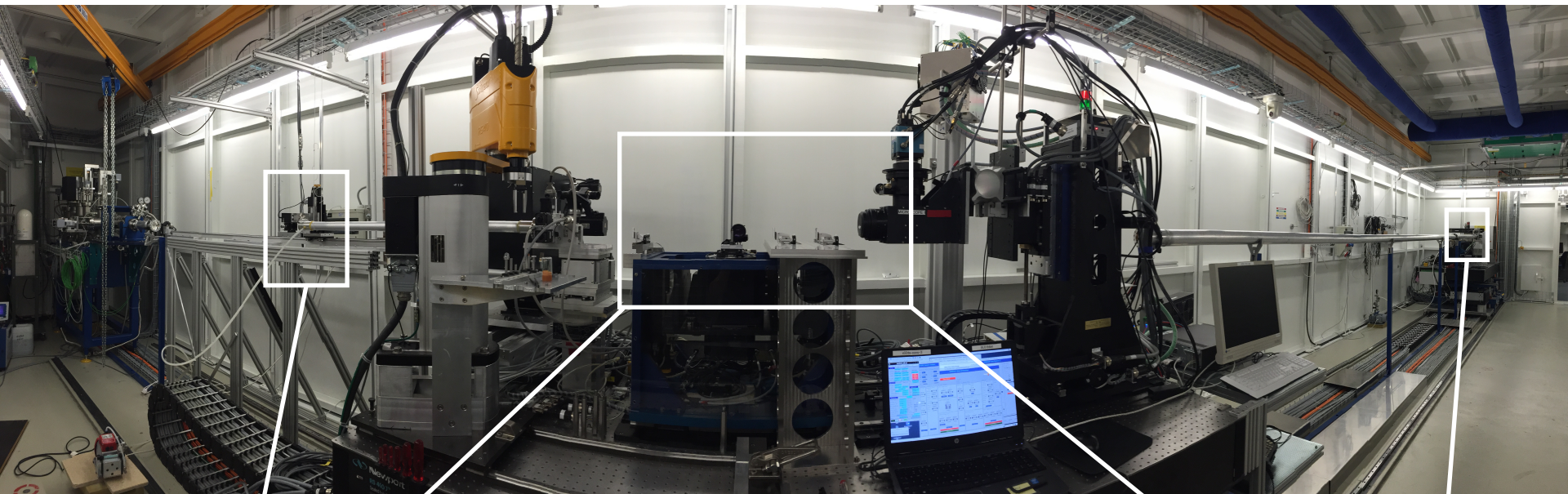
I. Vartiainen et al, Opt. Letters 2014

“Energy tunable” TOMCAT nanoscope (8-20 keV)

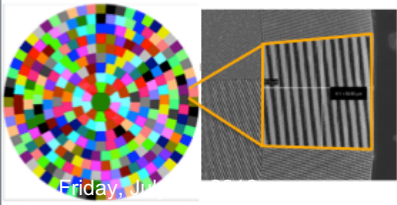
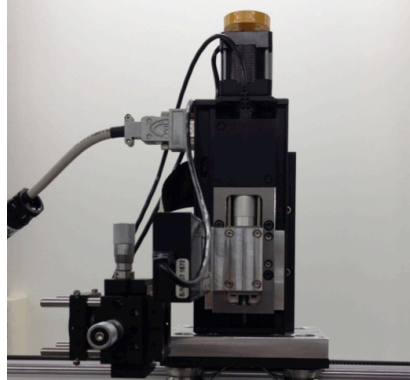


A. Bonnin

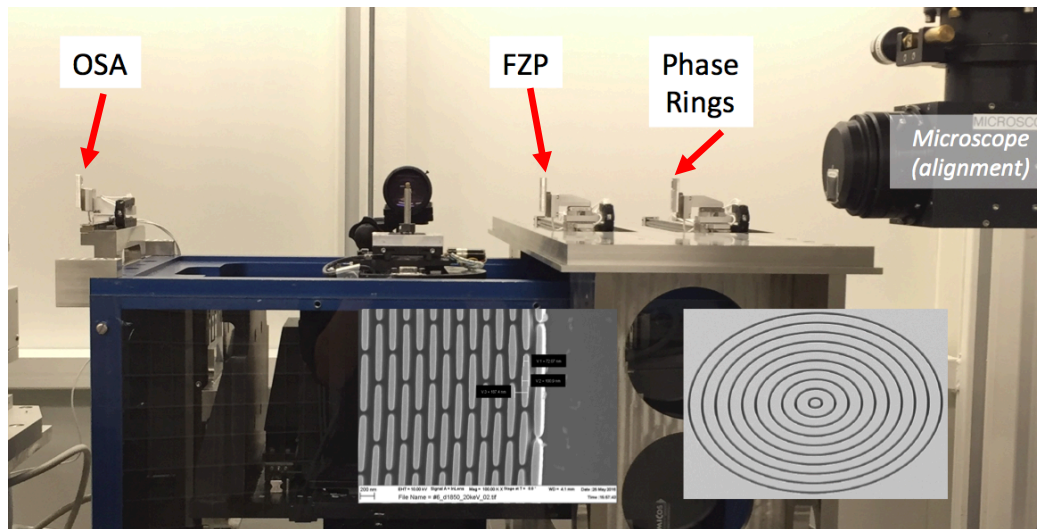
The “energy tunable” TOMCAT nanoscope



Moveable Condenser



Nanoscope optics



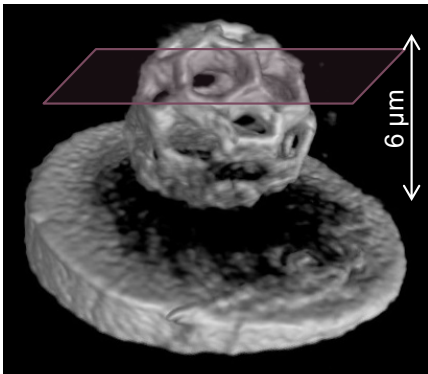
Detector



Custom PCO Edge 4.2
@ 10 m from FZP
magnification 80x
Effective pixel size 80nm

Cobalt-coated artificial buckyball polymer scaffold

3D artificial material composite:
cobalt-coated buckyball with about
270nm wall width.

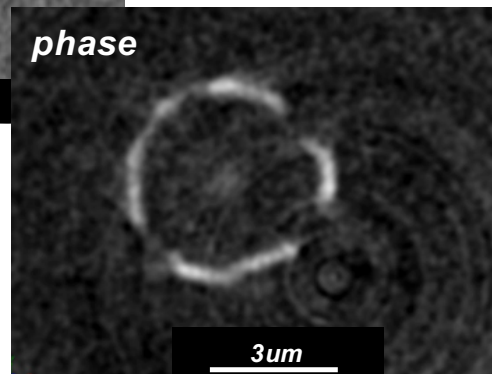
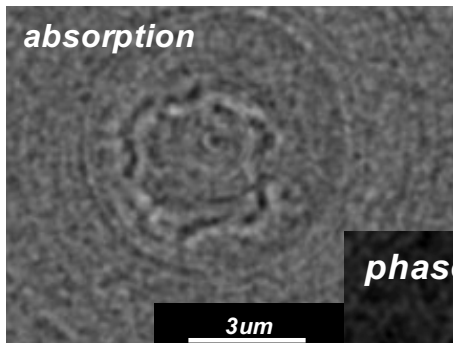


TOMCAT Nanoscope

Tomography scan:

- Si111 @ 12 keV
- Proj: 720
- Exp. Time: 3s
- Full chip!

→ 30 min scan!



PRL 114, 115501 (2015)

PHYSICAL REVIEW LETTERS

week ending
20 MARCH 2015

Element-Specific X-Ray Phase Tomography of 3D Structures at the Nanoscale

Claire Donnelly,^{1,2} Manuel Guizar-Sicairos,^{2,*} Valerio Scagnoli,^{1,2} Mirko Holler,² Thomas Huthwelker,² Andreas Menzel,² Ismo Vartiainen,² Elisabeth Müller,² Eugenie Kirk,^{1,2} Sebastian Gliga,^{1,2} Jörg Raabe,² and Laura J. Heyderman^{1,2,†}

¹Laboratory for Mesoscopic Systems, Department of Materials, ETH Zurich, 8093 Zurich, Switzerland

²Paul Scherrer Institute, 5232 Villigen PSI, Switzerland

(Received 23 October 2014; published 16 March 2015)

Recent advances in fabrication techniques to create mesoscopic 3D structures have led to significant developments in a variety of fields including biology, photonics, and magnetism. Further progress in these areas benefits from their full quantitative and structural characterization. We present resonant ptychographic tomography, combining quantitative hard x-ray phase imaging and resonant elastic scattering to achieve *ab initio* element-specific 3D characterization of a cobalt-coated artificial buckyball polymer scaffold at the nanoscale. By performing ptychographic x-ray tomography at and far from the Co *K* edge, we are able to locate and quantify the Co layer in our sample to a 3D spatial resolution of 25 nm. With a quantitative determination of the electron density we can determine that the Co layer is oxidized, which is confirmed with microfluorescence experiments.

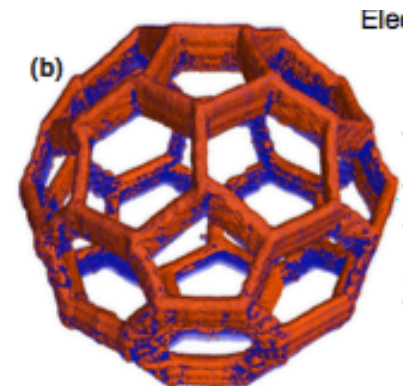
DOI: 10.1103/PhysRevLett.114.115501

PACS numbers: 81.07.-b, 42.30.Rx, 68.37.Yz, 81.70.Tx

Ptychographic Scan on cSAXS

- 3 min per projection
- 160 projections over 180°

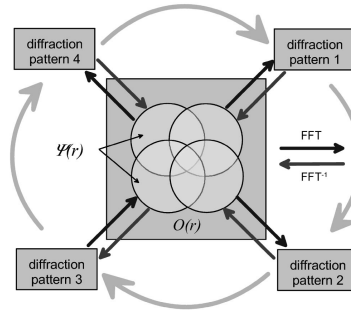
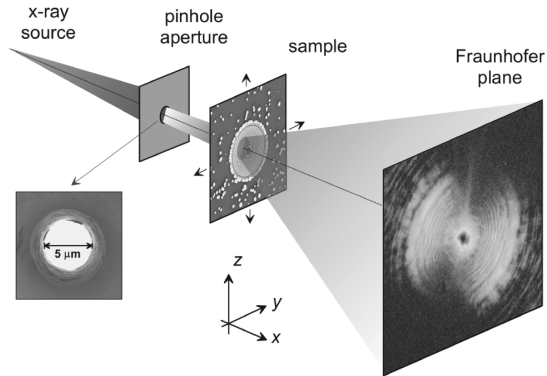
→ 8 h scan



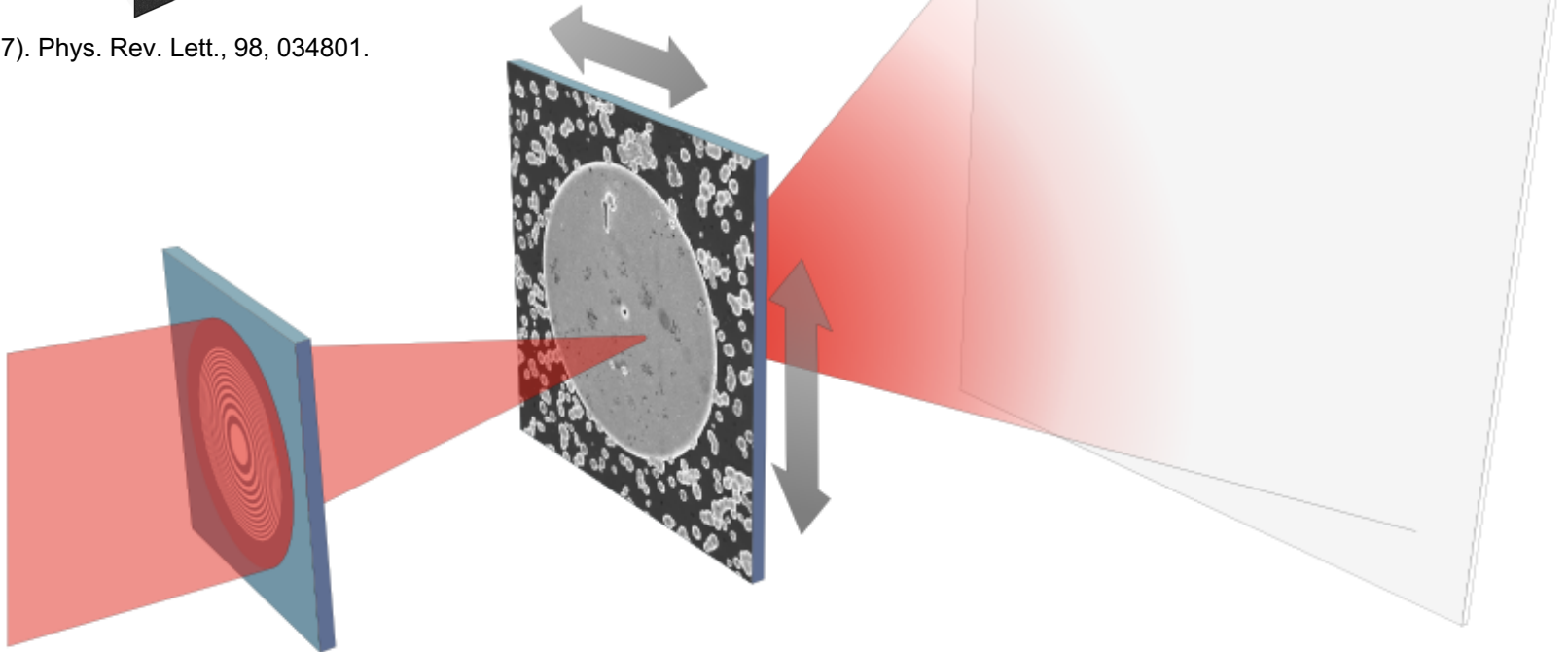
3D rendering with elemental contrast, where the Co is rendered in orange and the resist in blue.

Scanning X-ray diffraction microscopy

X-ray ptychography with a focused probe



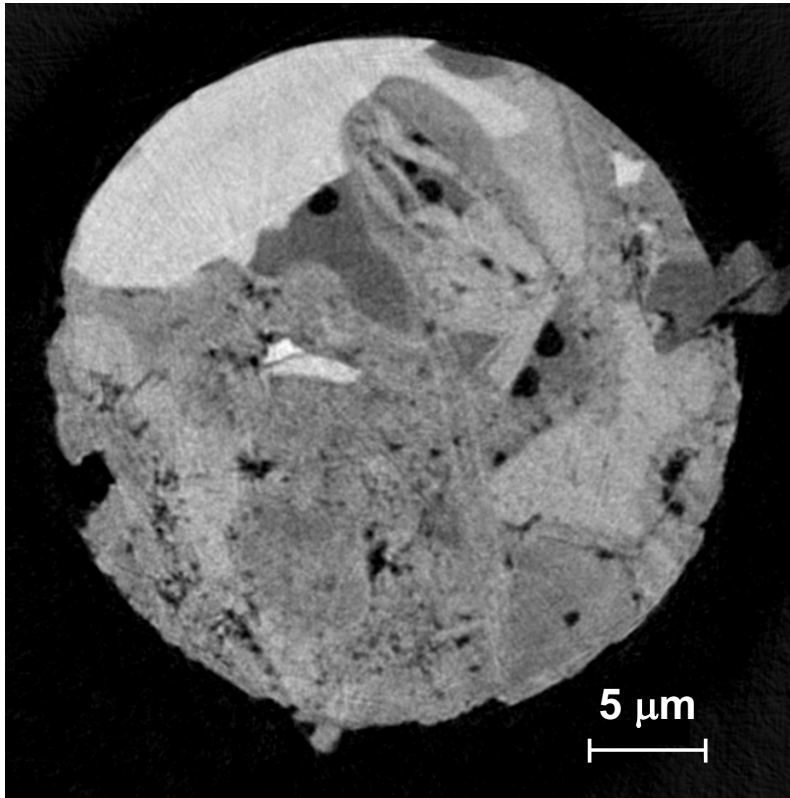
Rodenburg *et al.* (2007). Phys. Rev. Lett., 98, 034801.



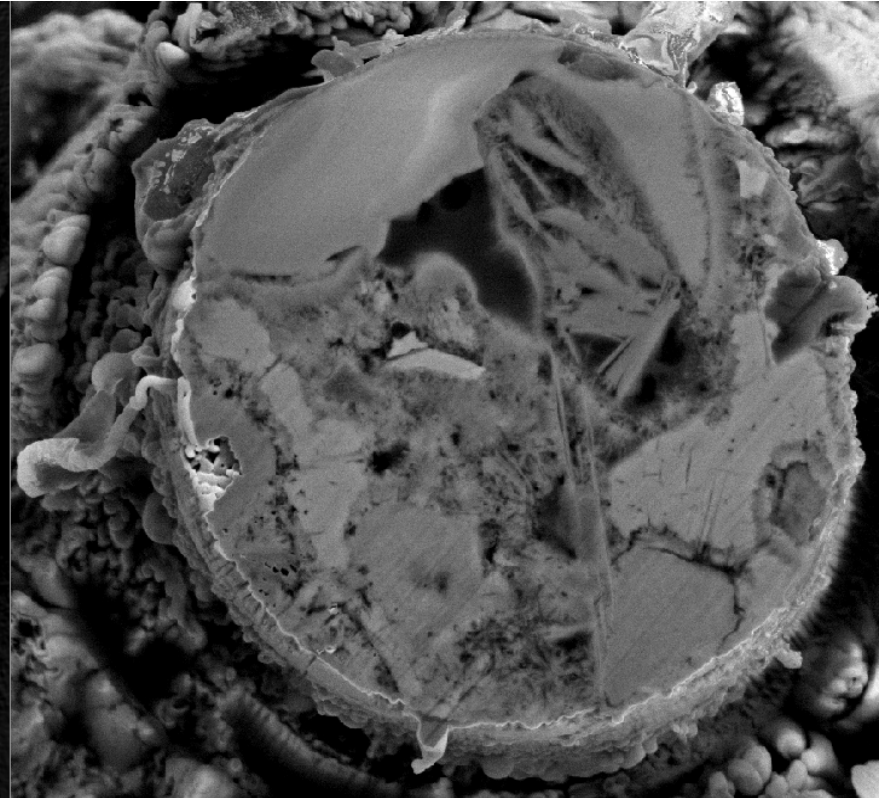
P. Thibault *et al.*, Science, 321, 379-382 (2008)

Ptychography on hardened cement paste

Ptycho-tomo

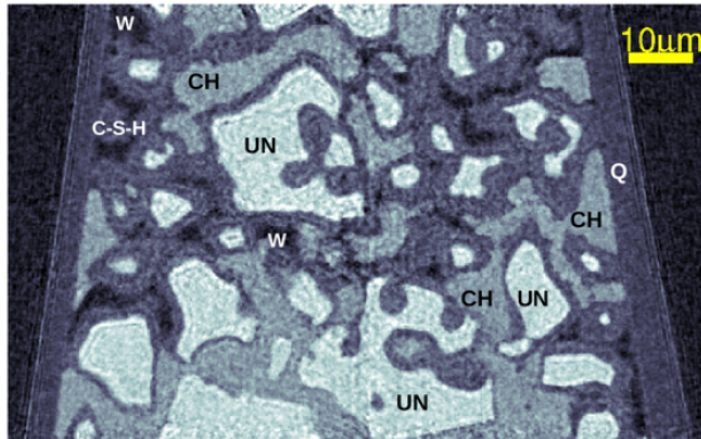


FIB-SEM



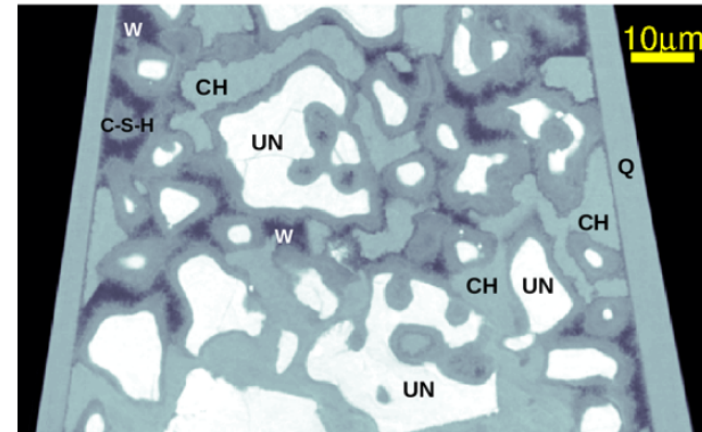
Hydrated cement paste

ABSORPTION



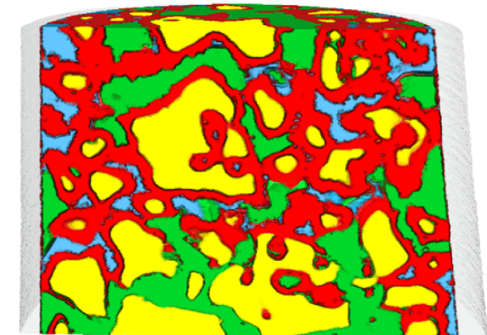
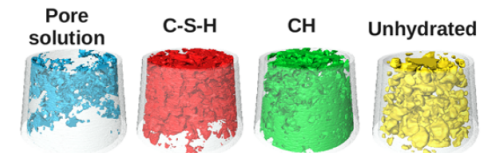
$\times 10^{-7}$
12
8 β
4
0

PHASE



$\times 10^{-5}$
1.6
1.2 δ
0.8
0.4
0

- Glass micro-capillary filled with hydrated cement phase
- Identification and segmentation of material phases:
 - UN: unhydrated alite particles
 - W: porosity comprising mostly water
 - CH: calcium hydroxide
 - C-S-H: calcium silicate hydrates
- Average mass density of C-S-H: 1.828 g/cm³

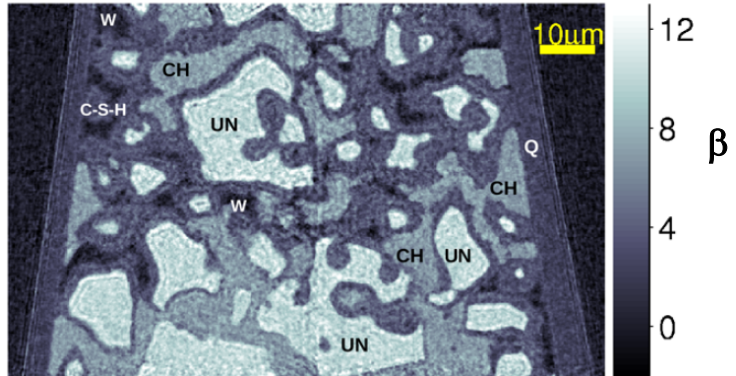


10 μm

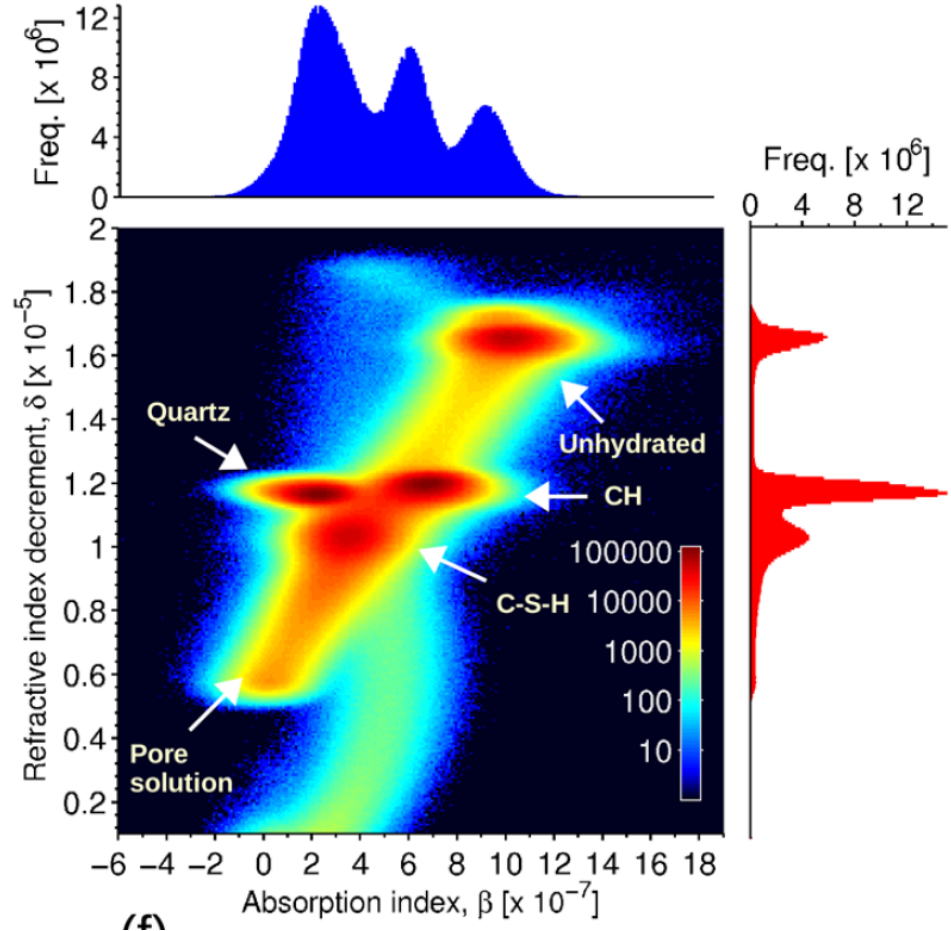
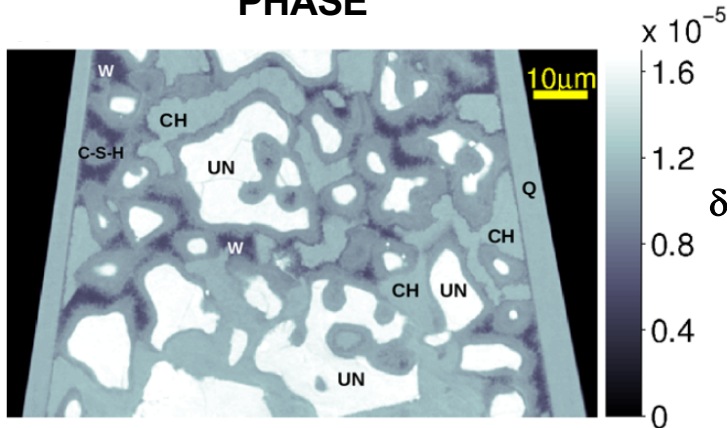
Slide courtesy of A. Diaz, cSAXS

Water content in hydrated cement paste

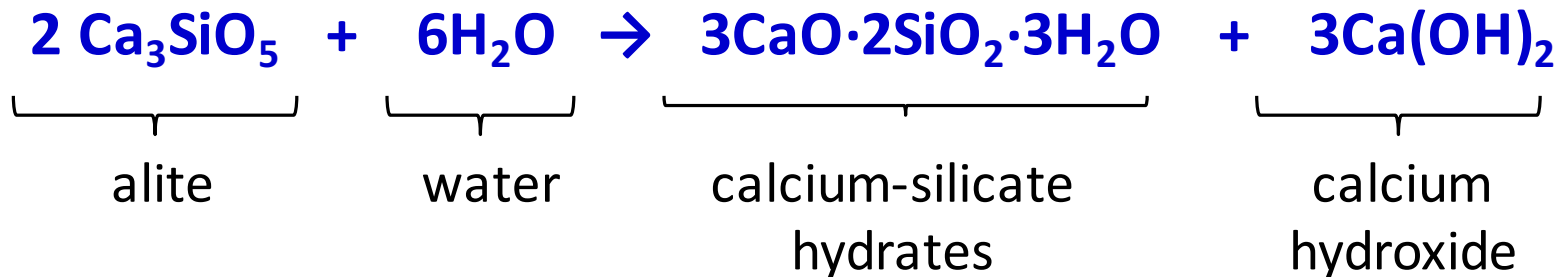
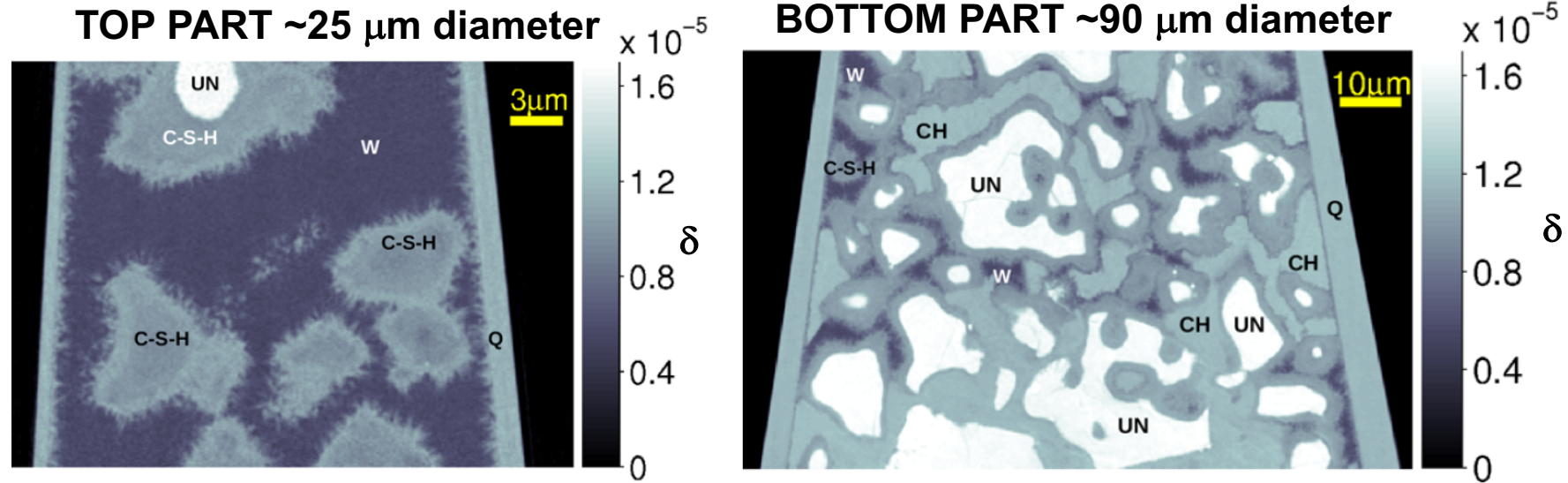
ABSORPTION



PHASE



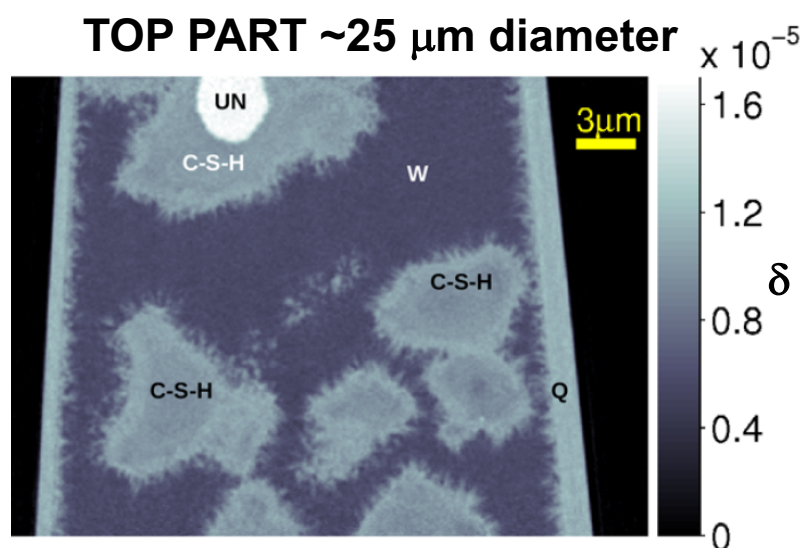
Hydrated cement paste



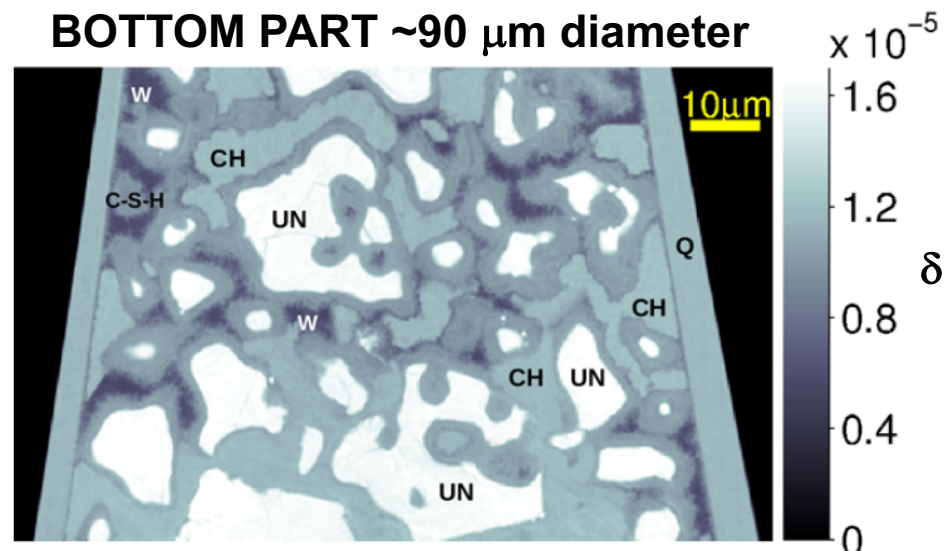
Glass micro-capillary filled with alite (C_3S) particles, flushed with water, sealed, and cured for 16 days

Hydrated cement paste

TOP PART ~25 μm diameter



BOTTOM PART ~90 μm diameter



CH: N/A

W: $(0.969 \pm 0.005) \text{ g/cm}^3$, theory: 1.000 g/cm^3

Q: $(2.158 \pm 0.002) \text{ g/cm}^3$, theory: 2.2 g/cm^3

C-S-H fully hydrated, inner: $(1.726 \pm 0.006) \text{ g/cm}^3$

C-S-H fully hydrated, outer: $(1.909 \pm 0.005) \text{ g/cm}^3$

C-S-H partly hydrated, inner: $(1.860 \pm 0.004) \text{ g/cm}^3$

C-S-H partly hydrated, outer: $(1.96 \pm 0.04) \text{ g/cm}^3$

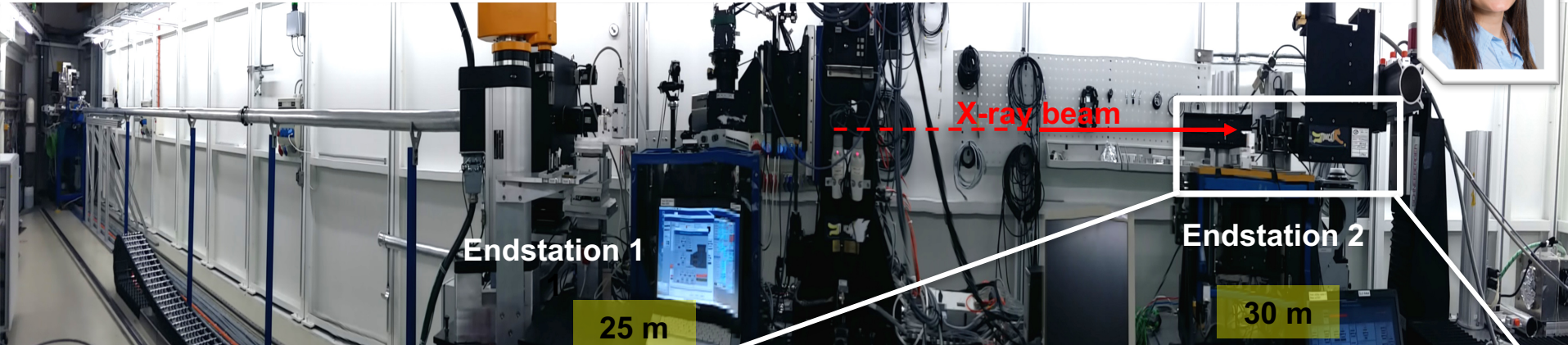
CH: $(2.184 \pm 0.004) \text{ g/cm}^3$, theory: 2.251 g/cm^3

W: $(0.994 \pm 0.005) \text{ g/cm}^3$, theory: 1.000 g/cm^3

Q: $(2.188 \pm 0.002) \text{ g/cm}^3$, theory: 2.2 g/cm^3

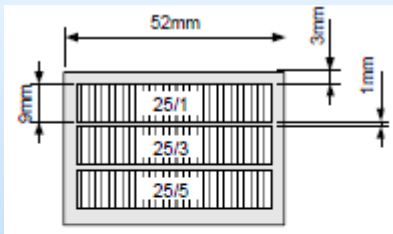
C-S-H, partly hydrated: $(1.828 \pm 0.005) \text{ g/cm}^3$

Grating interferometry at TOMCAT



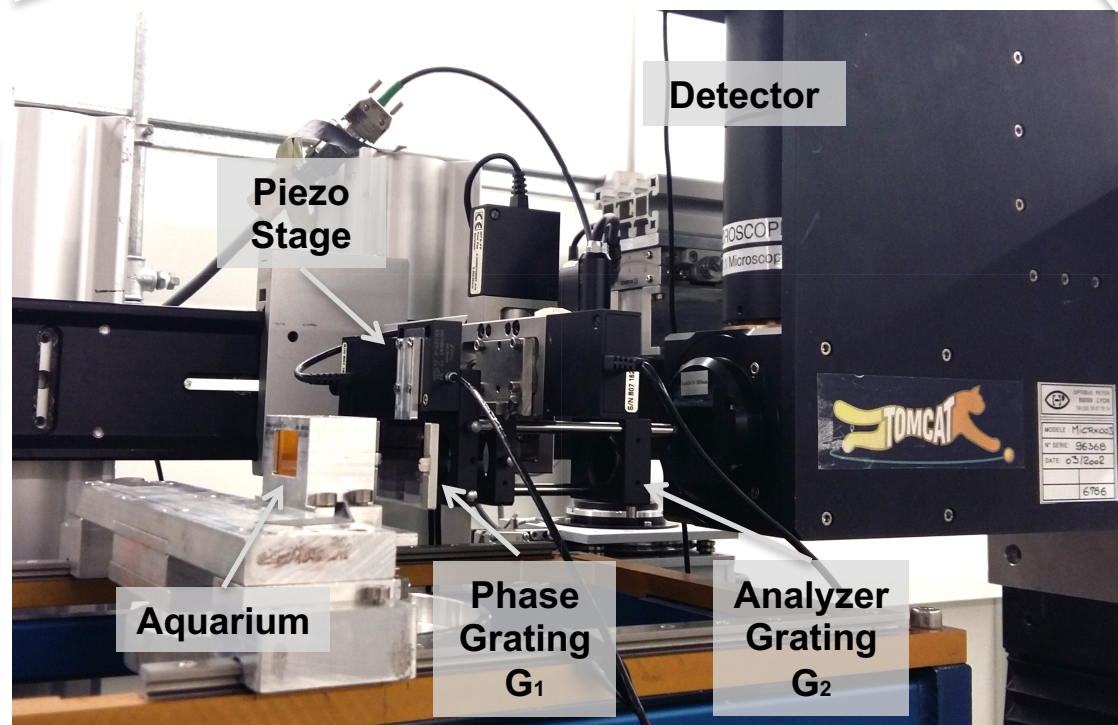
Phase Grating G_1

TO	Pitches [μm]
1	3.994
3	3.983
5	3.972



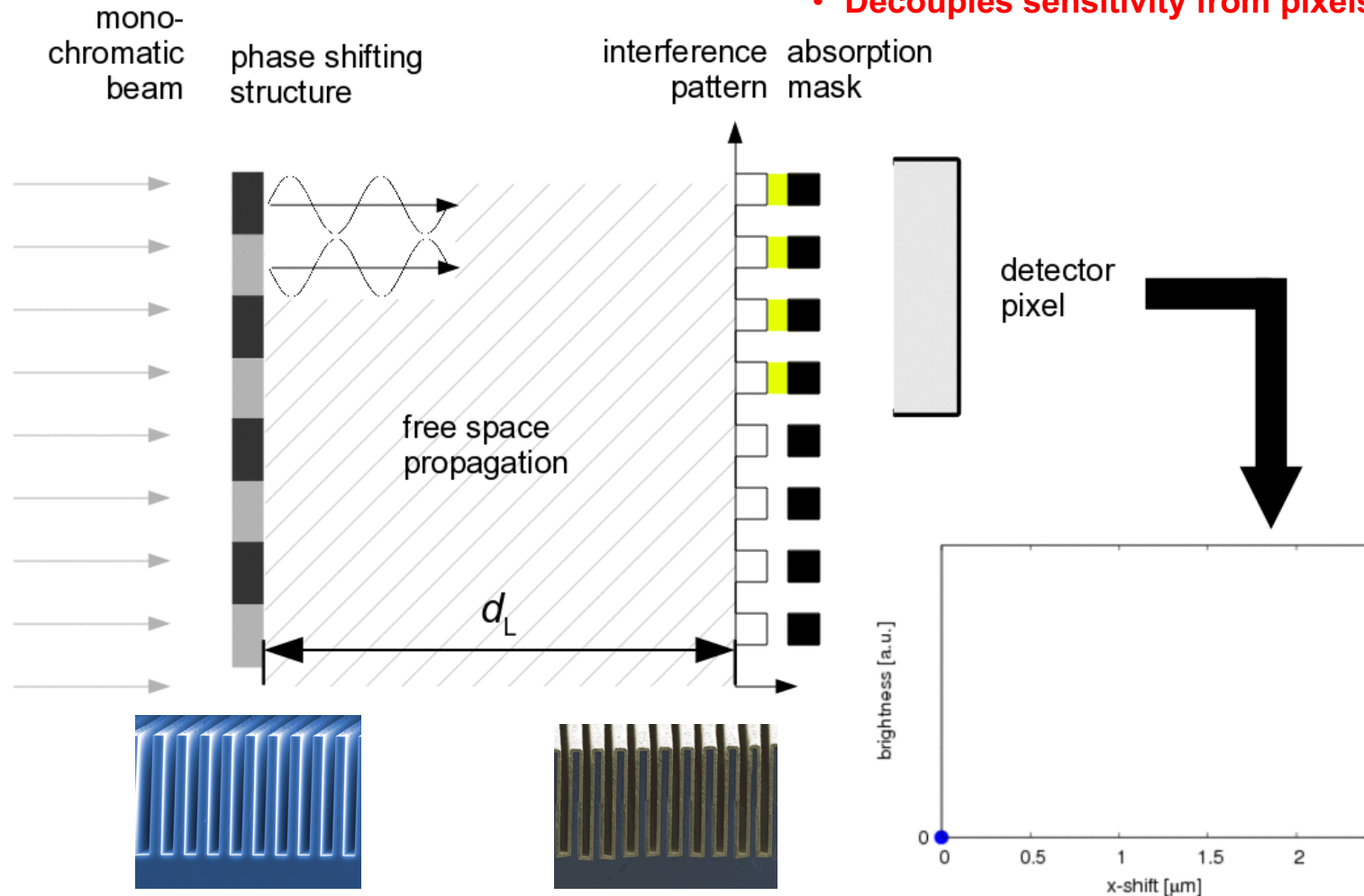
Phase shift of π .
Wafer thickness 250 μm .

Design energy = 25 keV
Other energies available on request



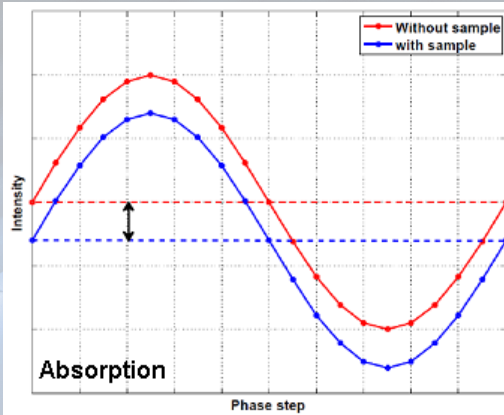
Grating interferometry in a nutshell

- Very sensitive on short distances
- Decouples sensitivity from pixelsize



Sensing the wavefront with grating interferometry

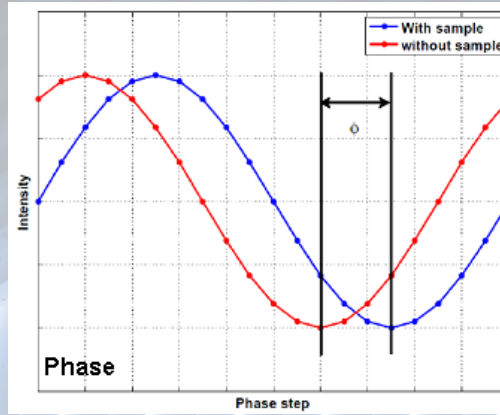
Absorption contrast



$$-\log\left(\frac{I_s}{I_b}\right)$$



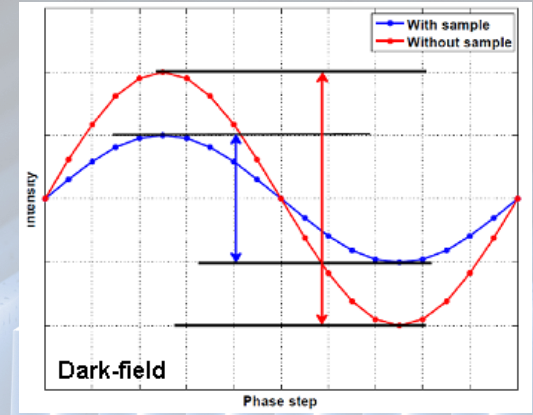
Differential phase contrast



$$\Phi_s - \Phi_b$$



Dark-field contrast



$$-\log\left(\frac{V_s}{V_b}\right) \quad V = \frac{I_{max} - I_{min}}{I_{max} + I_{min}}$$



Improved soft tissue contrast

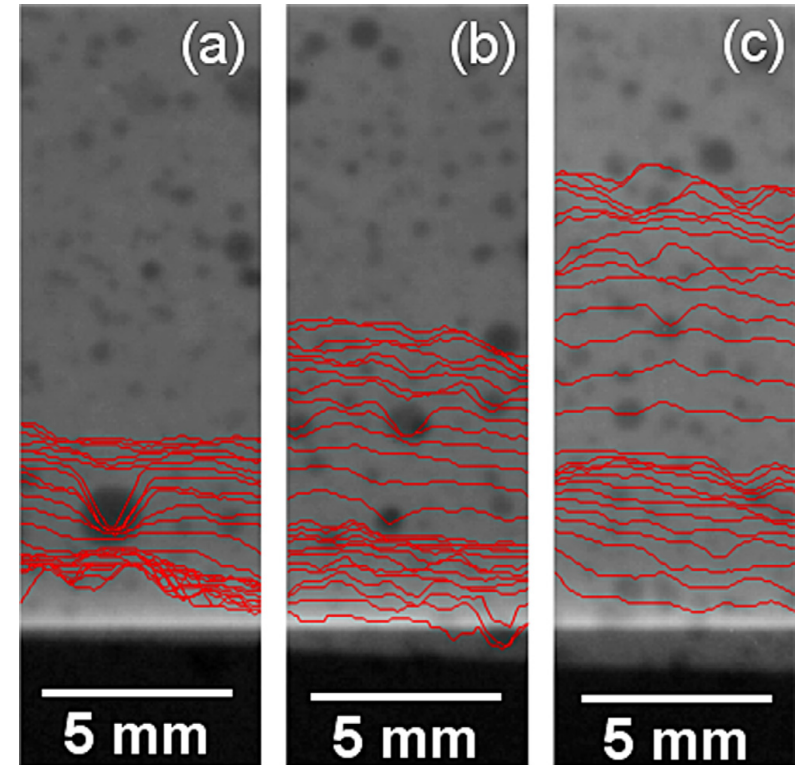
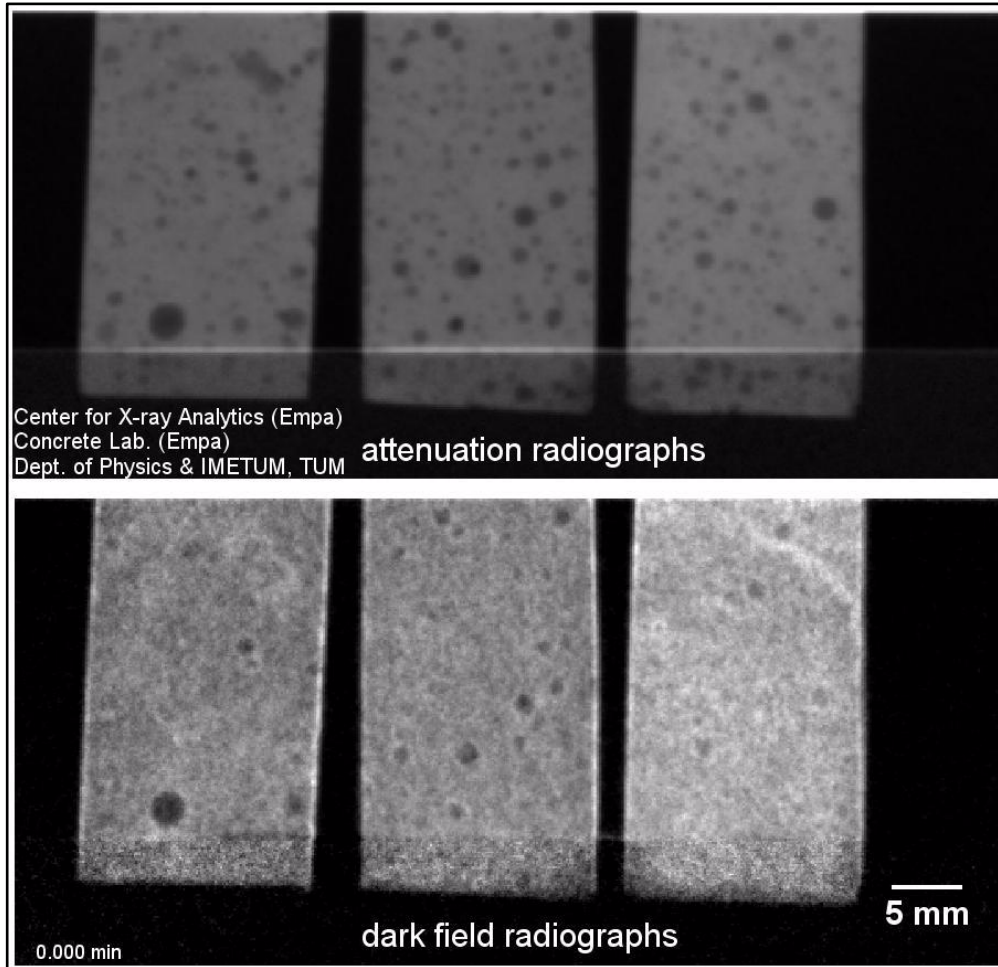
Phase

Absorption

Same dose

1 mm

Dark-field X-ray imaging of water capillary uptake in mortars

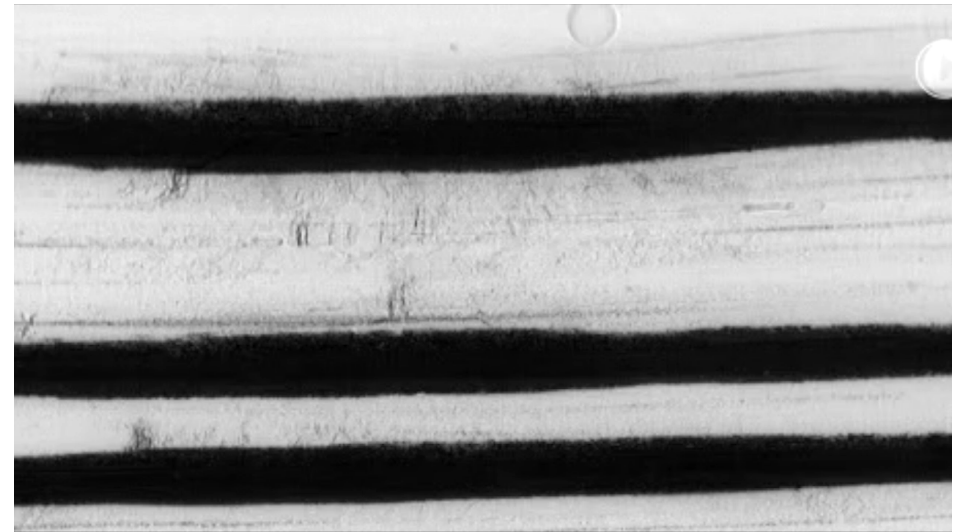
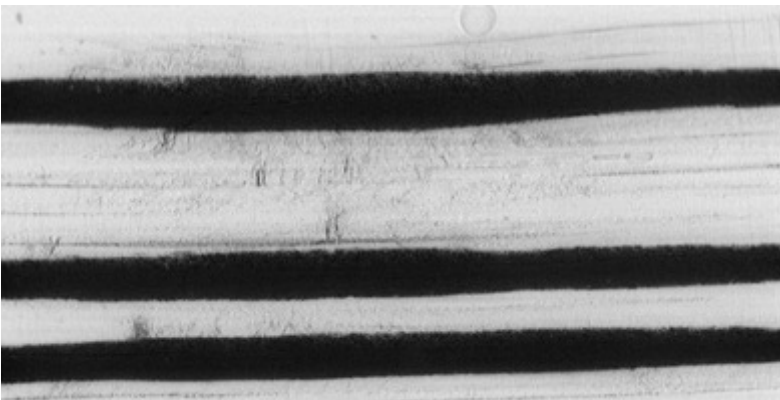
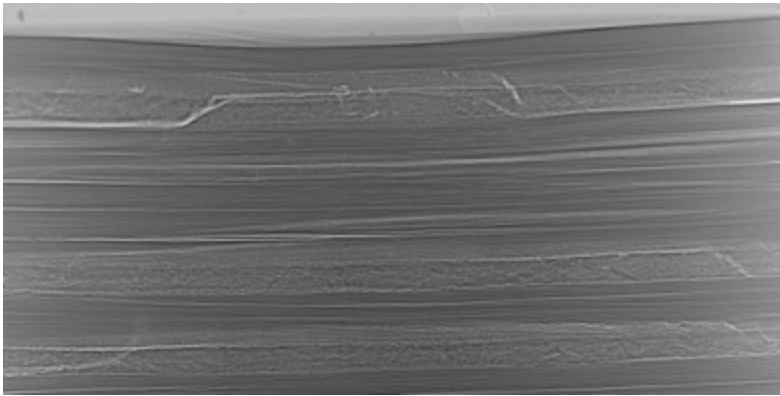


Wetting front positions (red lines) for three differently treated (heat load) samples.

F. Yang, et al. Appl. Phys. Lett. 105, 154105 (2014)

Darkfield radiology

CFRP laminated structure consisting of alternate layers of plastic matrix and fiber reinforcement



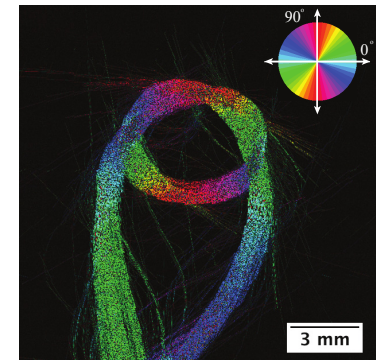
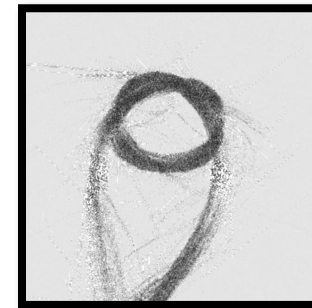
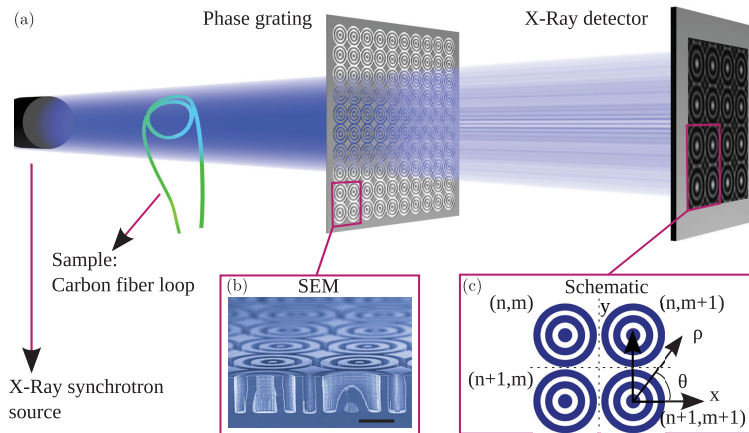
**Directional dependency of the darkfield signal.
Issues with the tomographic reconstruction...**



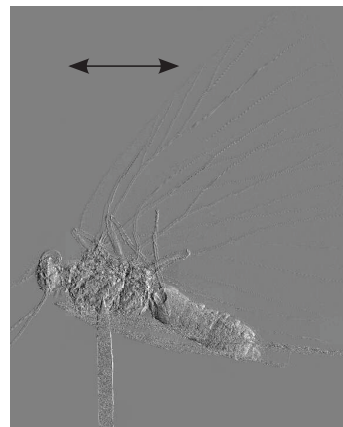
10 mm



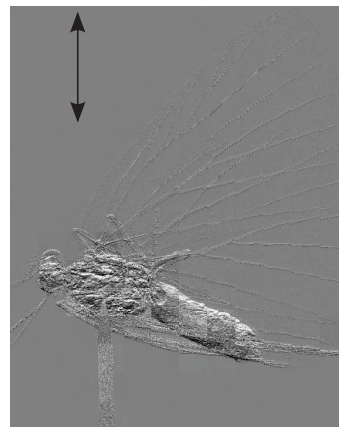
Single-shot 2D-omnidirectional hard X-ray scattering (dark-field) sensitivity



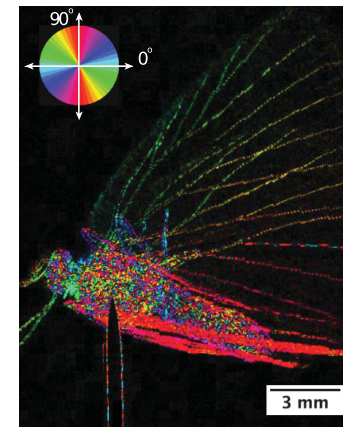
(a)



(b)



(c)



(d)

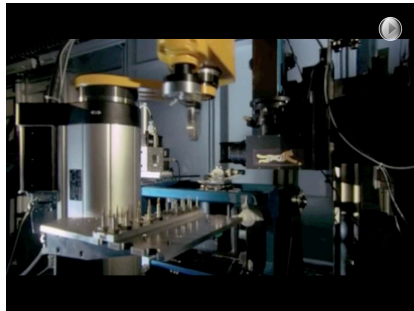
FIG. 3. (a) Absorption, (b) differential phase along x , (c) differential phase along y , and (d) directional scattering image of a butterfly fixed on a steel needle. The extracted scattering orientations are related to structures in the size range of the autocorrelation length of the system, which in our case is $2.5 \mu\text{m}$.

M. Kagias *et al.*, Phys. Rev. Lett. 116, 093902 (2016)

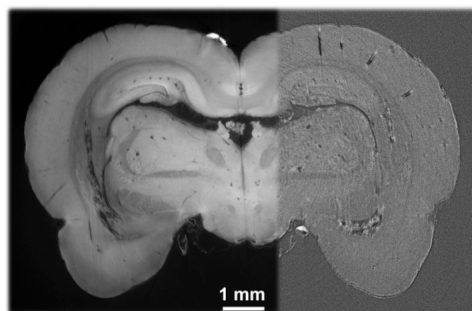
TOMCAT at a glance

Features:

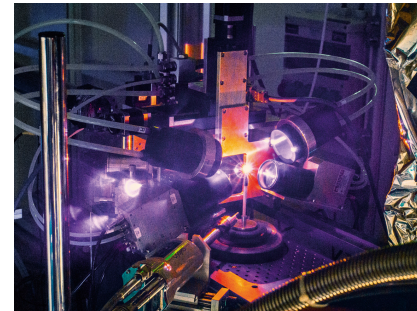
- Wide spatial resolution range: nano-to-meso scales (0.1-10 μ m)
- Broad range of sample sizes (10 μ m-20mm)
- High density resolution enhanced by phase contrast
- High temporal resolution (3D data acquisition in less than 1s)



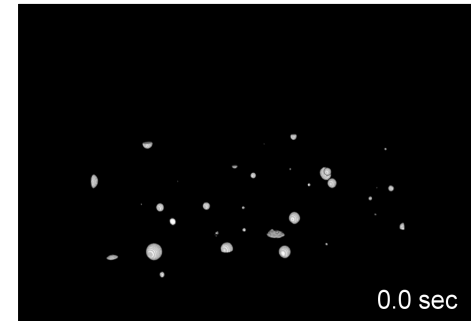
Automation
large scale
studies



Density resolution
phase contrast
imaging

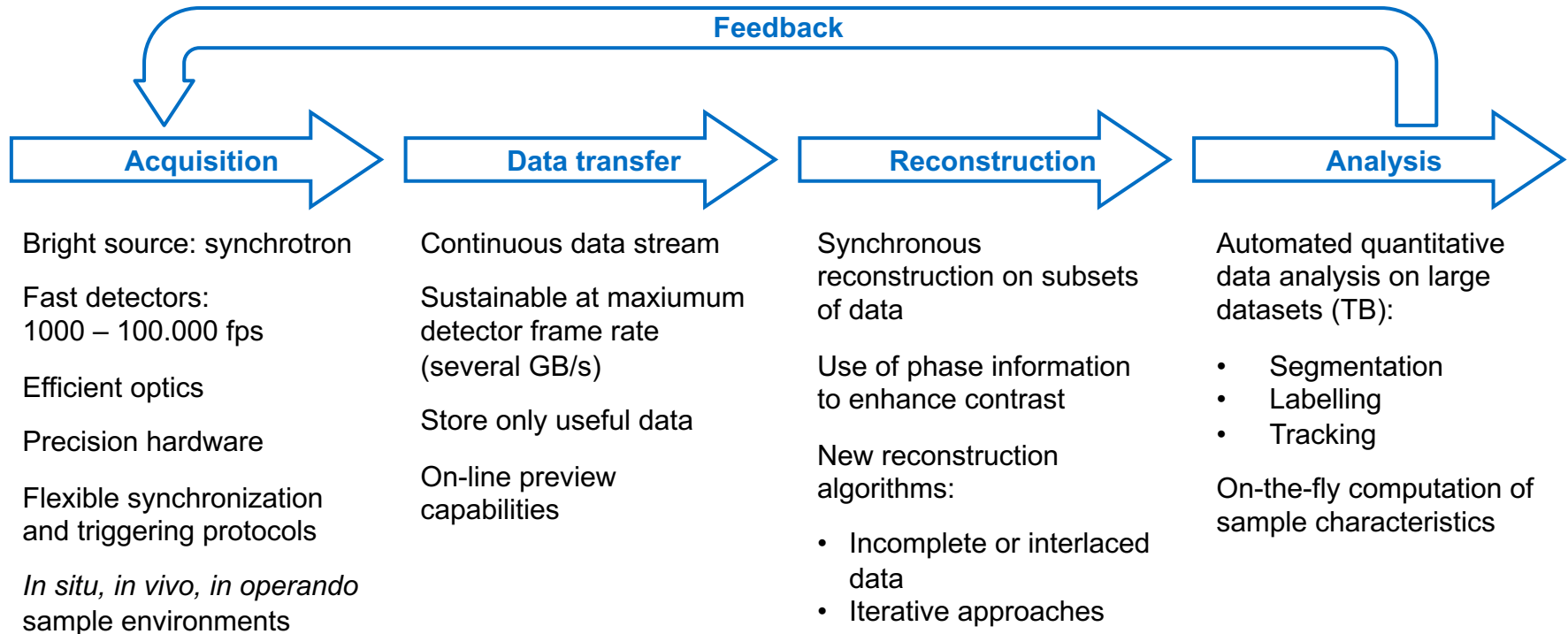


In situ
capabilities
temperatures
away from
ambient

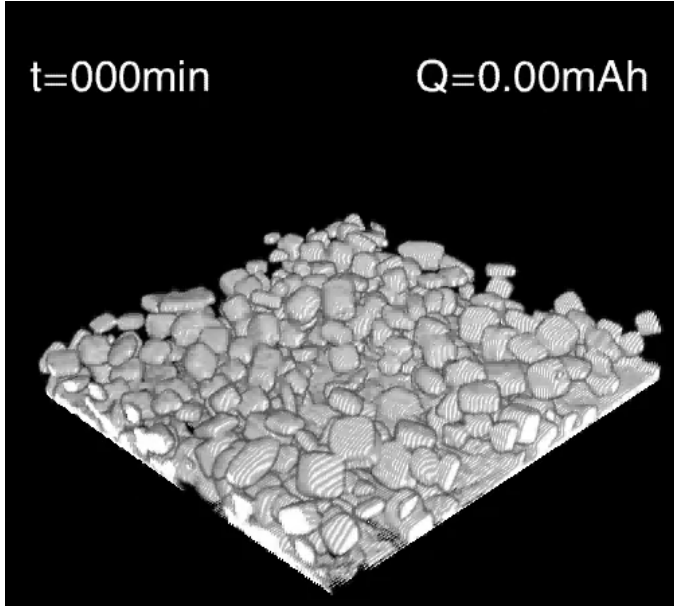
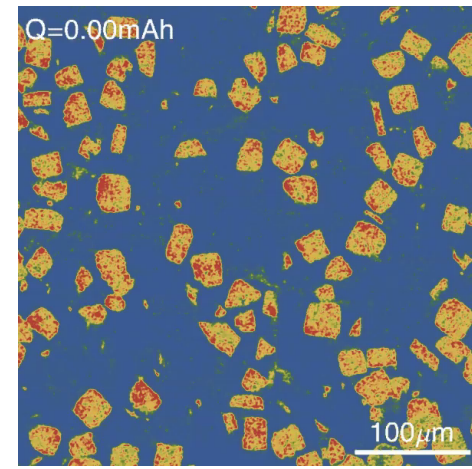
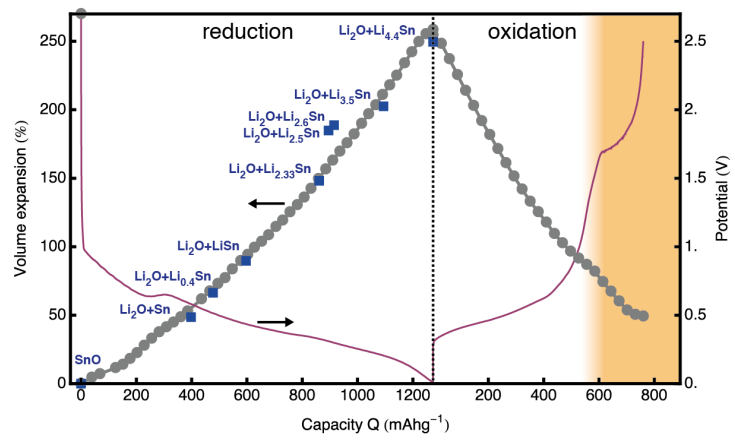
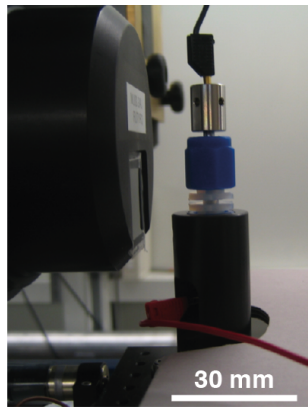


Ultra-fast data
acquisition
dynamic studies

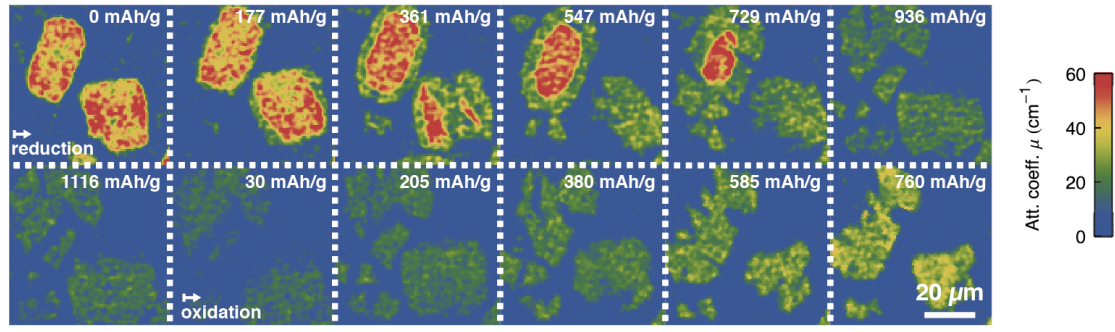
Requirements for fast tomography



In-operando tomography: catch the dynamics of your sample



- De-lithiation process in battery operation**
- Particle expansion
 - Monitoring of the reaction mechanism

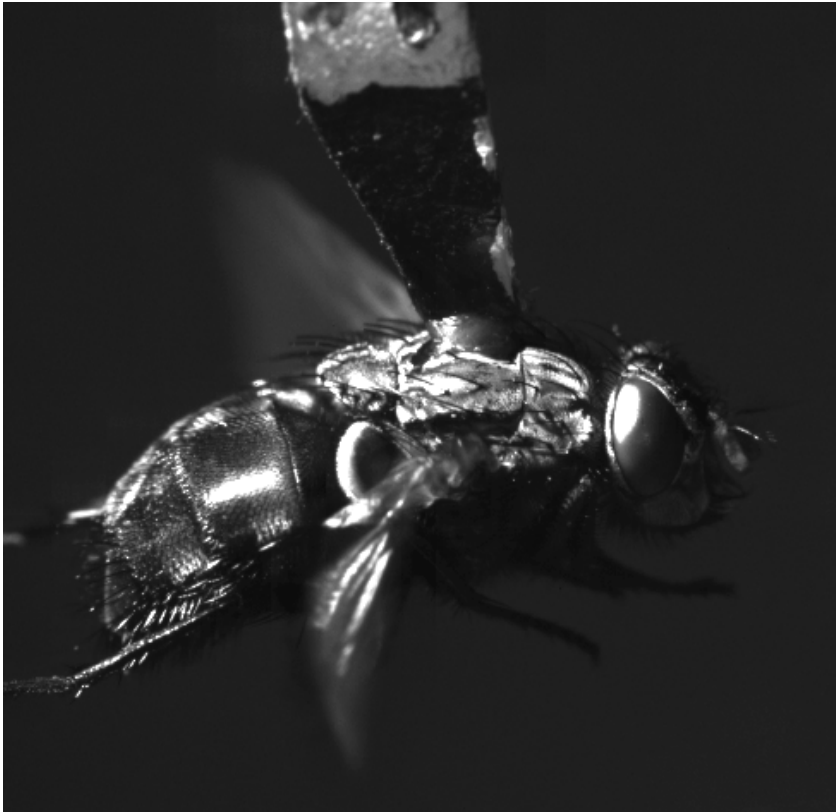


M. Ebner, F. Marone, M. Stampanoni, V. Wood, *Science* 342, 716 (2013)

Get insights in insect flight control

Investigate the biomechanics underlying flight manoeuvres and gaze shifts

→ **CT following the dynamics of 100+ Hz wing beat!**



- Time resolution way too demanding for standard CT data acquisition
 - BUT: Motion is quasi-periodic!
 - Resolve a time-averaged motion pattern over multiple wing beat periods?
- Gated kHz tomography
- kHz time resolution
 - Averaged motion over many cycles

The “fly” experiment

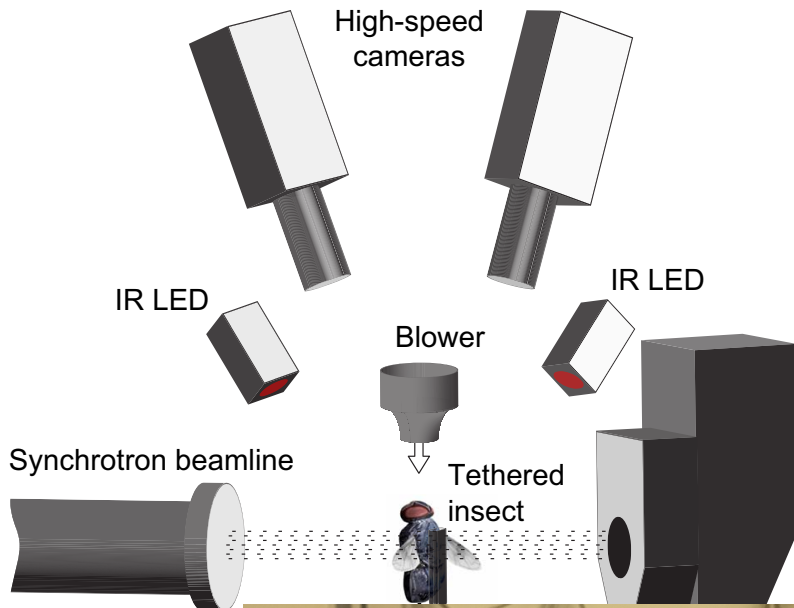
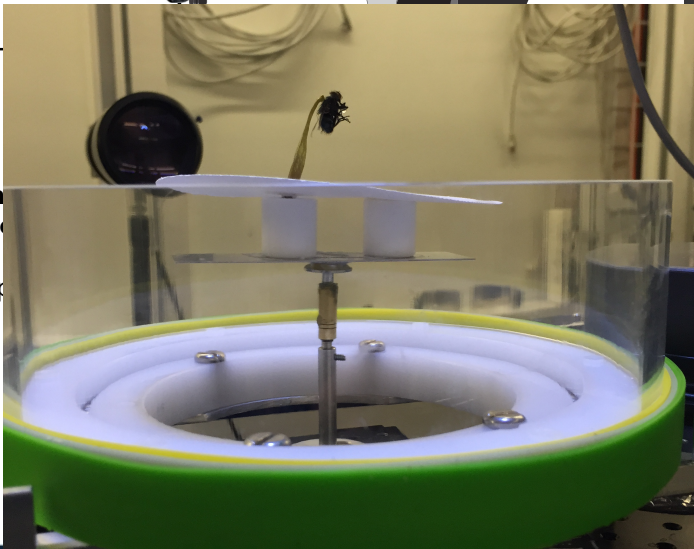


Figure 1. Schem showing the directional stimuli
doi:10.1371/journal.p



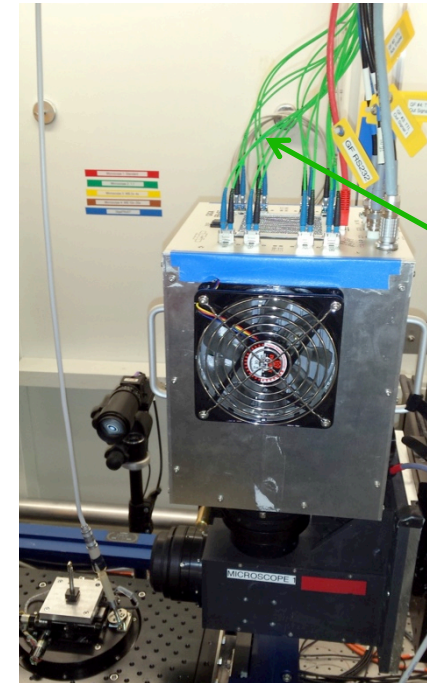
The fly's flight recorder...



- Limitations:
 - Fast acquisition into onboard memory
 - Total number of frames limited by memory
 - Data transfer to network storage MUCH slower than measurement
(Dimax: few seconds dataset, 45 min transfer)
- Implications:
 - Fast acquisition only for short periods
 - Blind acquisition → Need to know exactly when to look
 - Reduce FOV to increase number of frames
 - Many phenomena cannot be studied in full length

GigaFRoST : Gigabit Fast Read-Out System for Tomography

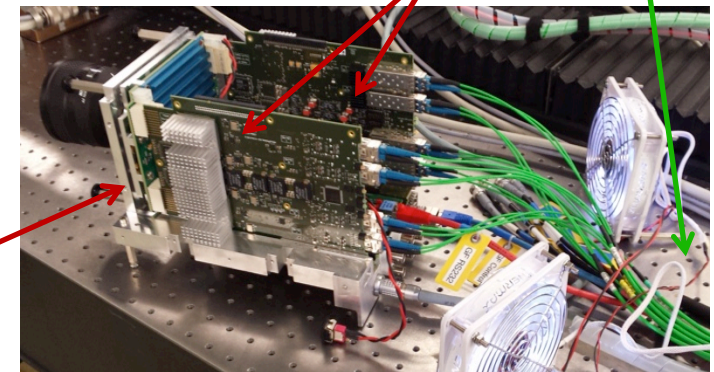
- PSI in-house development
- In user operation since September 2015
- pco.Dimax fast imaging sensor
- Custom readout electronics
- No on-board memory
- 8 parallel fiber-optic connections, continuous direct data streaming to server:
8 GB/s → 1 TB/2min!
- 1.25 kHz full frame rate (2016x2016 @ 12 bit)
10 kHz @ 576x575, 12 bit
- Live preview from subset of streamed images



fiber-optic connections

GigaFRoST data boards

pco.Dimax headboard



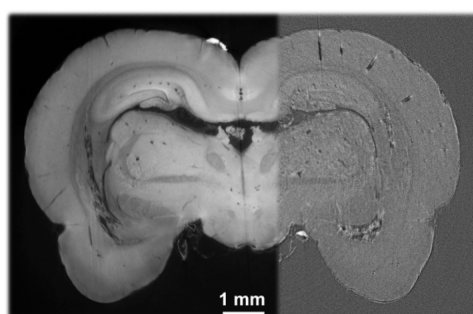
TOMCAT at a glance

Features:

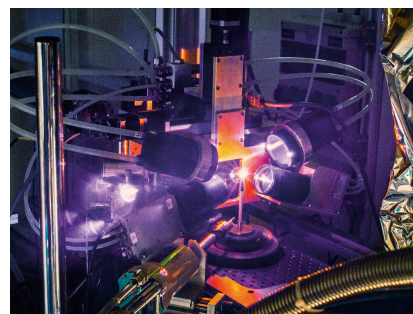
- Wide spatial resolution range: nano-to-meso scales (0.1-10 μ m)
- Broad range of sample sizes (10 μ m-20mm)
- High density resolution enhanced by phase contrast
- High temporal resolution (3D data acquisition in less than 1s)



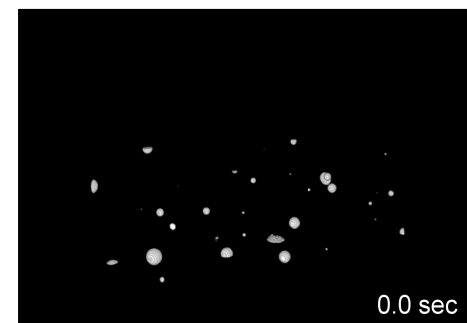
Automation
large scale
studies



Density resolution
phase contrast
imaging

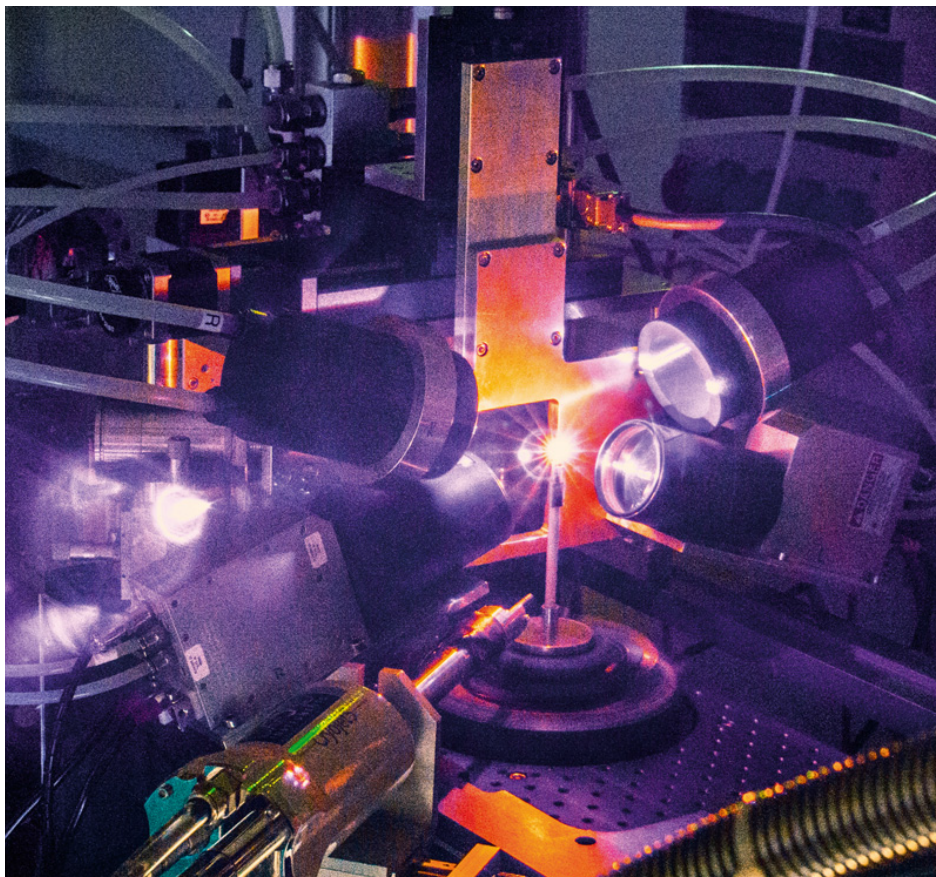


In situ
capabilities
temperatures
away from
ambient

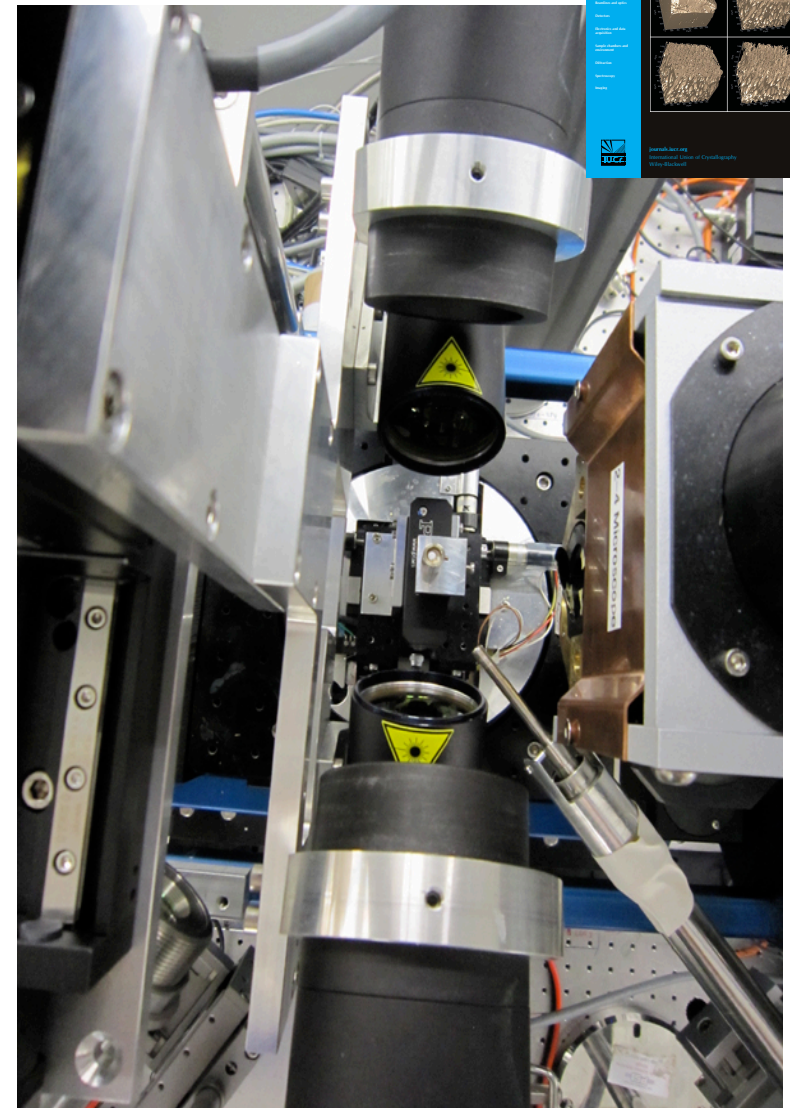


Ultra-fast data
acquisition
dynamic studies

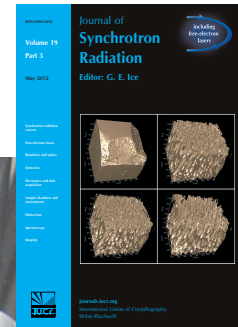
Laser Furnace



- 2 cross firing 150W, 980nm cw, class 4 lasers
- Temperature feedback with pyrometer
- Laser power and temperature control fully integrated.



J. Fife et al., Journal of Synchrotron Radiation 19(3), 352–358 (2012)



Crack propagation dynamics under tensile load @ 20 Hz

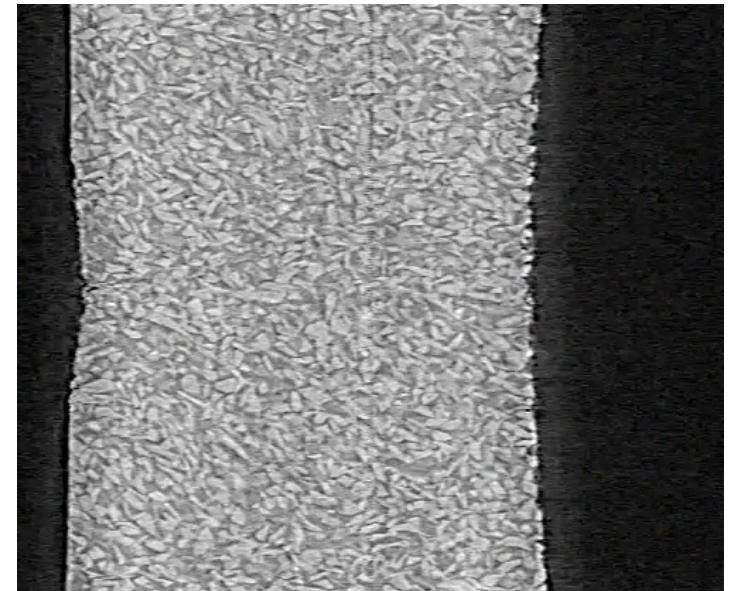
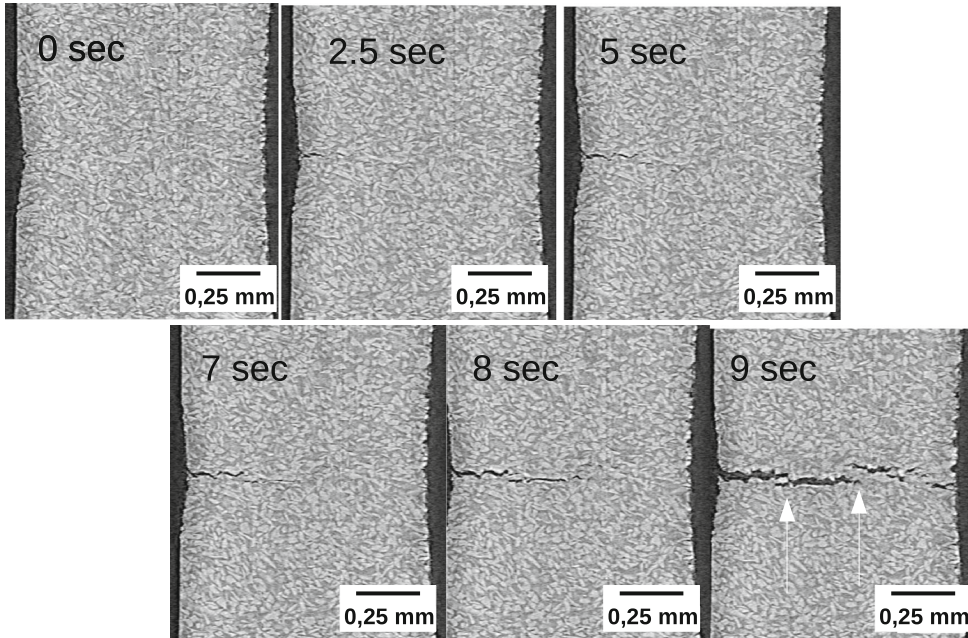
- Custom tensile rig
- Alumina particle reinforced aluminium composite
- Tomography:
 - Polychromatic beam (50% filter, mean energy 30 keV)
 - 100 μ s exposure time
 - 500 projections / scan
 - 50 ms scan time (20 Hz)
 - Sample rotating at 600 rpm



- **Fastest scans at TOMCAT to date!**

E. Maire, et. al., Int J Fract 1 (2016)

In-situ 20 Hz tomographic imaging

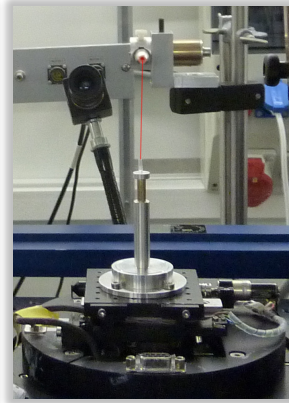
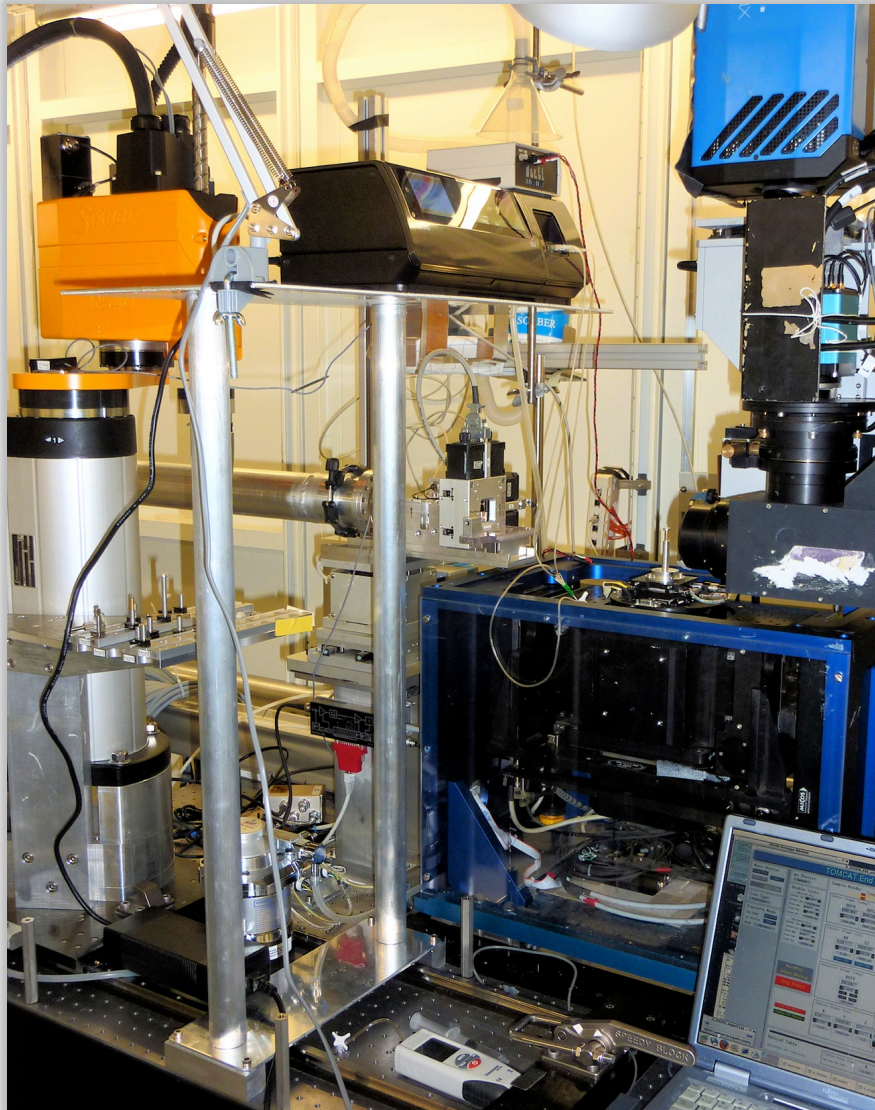


Movie playing in real time (9 seconds, 180 frames)



**E. Maire, INSA-Lyon, UCBL, CNRS, MATEIS
Université de Lyon France**

Dynamic 3D imaging in-vivo: complex triggering



Lovric et al., Physica Medica, 2016



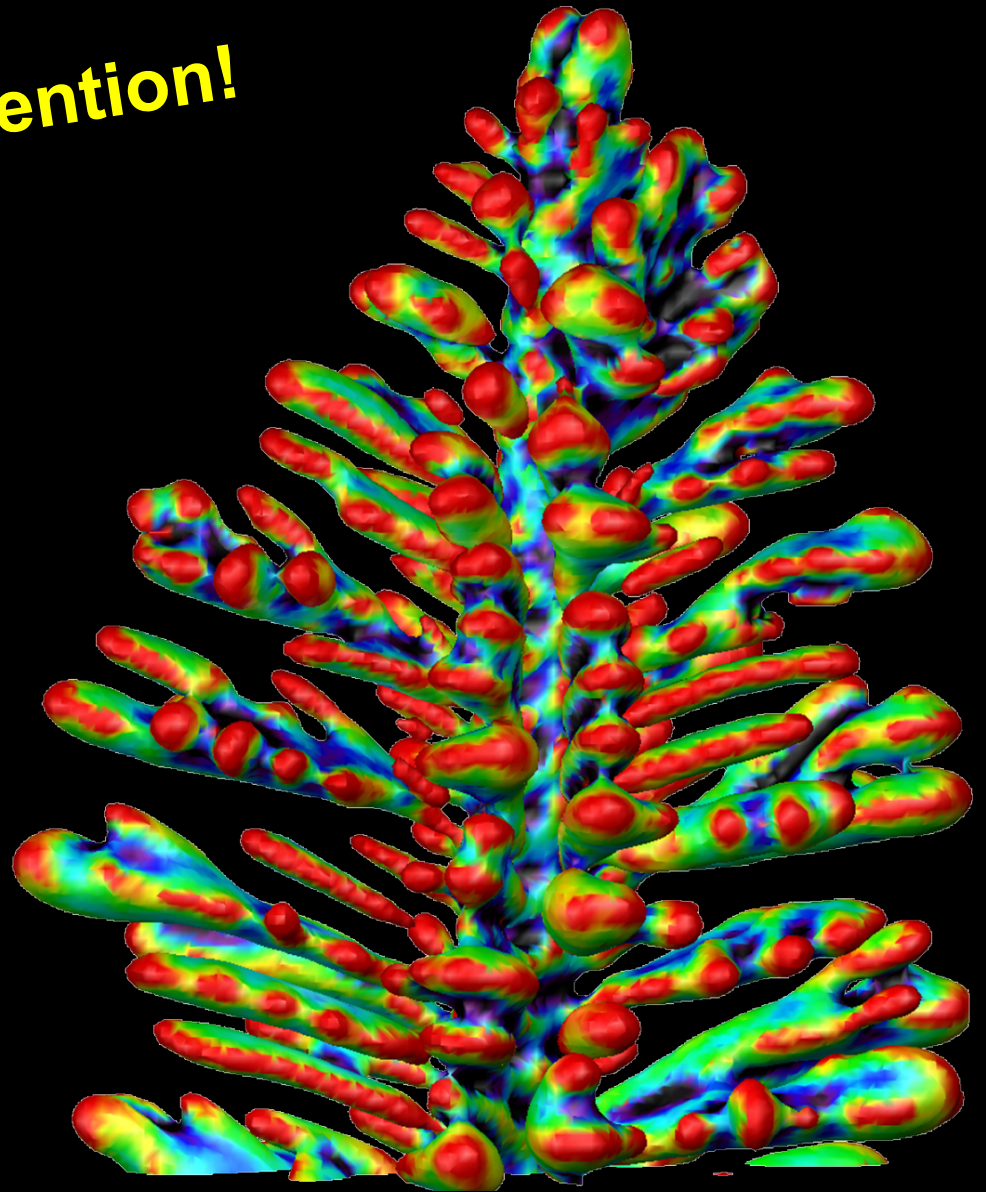
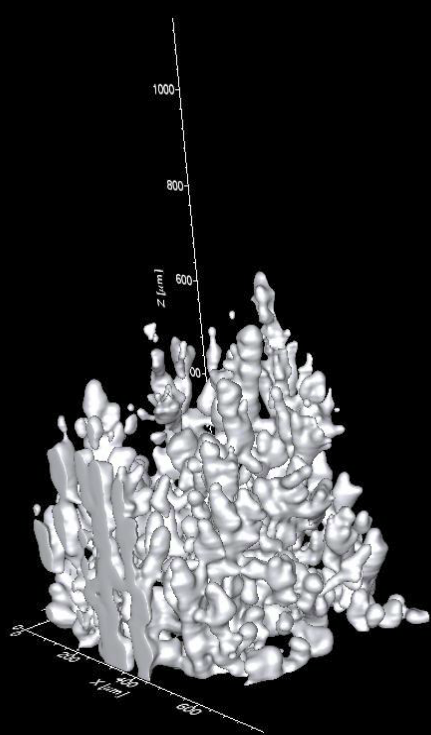
Summary

- TOMCAT offers high spatial and temporal resolutions in multiple modalities over a range of length scales
- “Unique” capabilities coupling sub-second AND continuous 3D data acquisition (GIGAFROST detector)
 - Removes hardware limitations that are present in other detector systems for observation of true dynamic phenomena
- Setup is ideal for time-resolved (4D) in-situ materials and in-vivo biological applications
- Cutting-edge grating-interferometry endstation for new microscopy applications and benchmarking purposes
- **Outlook: SLS2.0 with more flux , higher energies, round source.**

TOMCAT (flying) team



Thank you for your attention!



4D directionally solidified dendrites

Mean curvature colored dendrite (Al/Cu alloy)

J. Fife *et al.*, *in preparation*